# REPORT DOCUMENTATION PAGE

Form Approved
OMB No 0704-0188



| 1. AGENCY USE ONLY (Leave blank) | 2. REPORT DATE | 3. REPORT TYPE AND DATES COVERED |
|---|---|---|
| | 1993 | THESIS/DISSERTATION |

**4. TITLE AND SUBTITLE**
A FLOW VISUALIZATION STUDY OF ACOUSTICALLY ENHANCED HAIRPIN VORTICES

**5. FUNDING NUMBERS**

AD-A275 467

**6. AUTHOR(S)**
STEPHEN A. WHYTE

**7. PERFORMING ORGANIZATION NAME(S) AND ADDRESS(ES)**
AFIT Student Attending: UNIVERSITY OF WASHINGTON

**8. PERFORMING ORGANIZATION REPORT NUMBER**
AFIT/CI/CIA- 93-164

**9. SPONSORING/MONITORING AGENCY NAME(S) AND ADDRESS(ES)**
DEPARTMENT OF THE AIR FORCE
AFIT/CI
2950 P STREET
WRIGHT-PATTERSON AFB OH 45433-7765

**10. SPONSORING/MONITORING AGENCY REPORT NUMBER**

**11. SUPPLEMENTARY NOTES**

**12a. DISTRIBUTION/AVAILABILITY STATEMENT**
Approved for Public Release IAW 190-1
Distribution Unlimited
MICHAEL M. BRICKER, SMSgt, USAF
Chief Administration

**12b. DISTRIBUTION CODE**

**13. ABSTRACT** (Maximum 200 words)

94-03965



94 2 03 179

| 14. SUBJECT TERMS | 15. NUMBER OF PAGES 53 |
|---|---|
| | 16. PRICE CODE |

| 17. SECURITY CLASSIFICATION OF REPORT | 18. SECURITY CLASSIFICATION OF THIS PAGE | 19. SECURITY CLASSIFICATION OF ABSTRACT | 20. LIMITATION OF ABSTRACT |
|---|---|---|---|
| | | | |

93-164

**University of Washington**

Abstract

A Flow Visualization Study of Acoustically
Enhanced Hairpin Vortices
by Stephen A. Whyte

Chairperson of the Supervisory Committee:
Professor Mitsuru Kurosaka
Department of Aeronautics and Astronautics

For many years the turbulent boundary layer was thought to be composed of totally chaotic and random eddies. However, recent work has shown that a very organized array of structures exist in this regime. These structures, named hairpin, horseshoe or Λ- shaped vortices, compose a major portion of the turbulent boundary layer and may be responsible for the increased heat transfer seen in turbulent regimes.

The hairpin vortex is a vortex line that has been lifted off of the surface and through mutual induction of its legs forms a loop. This loop is composed of two counter-rotating legs, oriented at 45 degrees to the wall, with a head that joins the two legs together. These legs act like tornados sweeping along the wall. They transport air adjacent to the wall up through the legs and into the head. Research at the University of Washington has shown that this 'tornado effect' increased the heat flux away from the wall. If this capability can be harnessed and enhanced, the effects of film cooling in turbine engines can be dramatically increased.

Earlier research at the U of W has demonstrated the effects of a single hairpin; however, the effect of the hairpin array are not understood. This thesis presents new theories into hairpin array growth with the goal of acoustic enhancement of the array structure. Research in a turbulent boundary layer has given initial confirmation of the array theories developed in this paper through flow visualization. Acoustic enhancement was also accomplished through low frequency white noise excitation of the hairpin vortex array.

**University of Washington**

## Abstract

A Flow Visualization Study of Acoustically
Enhanced Hairpin Vortices
by Stephen A. Whyte

Chairperson of the Supervisory Committee:
Professor Mitsuru Kurosaka
Department of Aeronautics and Astronautics

For many years the turbulent boundary layer was thought to be composed of totally chaotic and random eddies. However, recent work has shown that a very organized array of structures exist in this regime. These structures, named hairpin, horseshoe or Λ- shaped vortices, compose a major portion of the turbulent boundary layer and may be responsible for the increased heat transfer seen in turbulent regimes.

The hairpin vortex is a vortex line that has been lifted off of the surface and through mutual induction of its legs forms a loop. This loop is composed of two counter-rotating legs, oriented at 45 degrees to the wall, with a head that joins the two legs together. These legs act like tornados sweeping along the wall. They transport air adjacent to the wall up through the legs and into the head. Research at the University of Washington has shown that this 'tornado effect' increased the heat flux away from the wall. If this capability can be harnessed and enhanced, the effects of film cooling in turbine engines can be dramatically increased.

Earlier research at the U of W has demonstrated the effects of a single hairpin; however, the effect of the hairpin array are not understood. This thesis presents new theories into hairpin array growth with the goal of acoustic enhancement of the array structure. Research in a turbulent boundary layer has given initial confirmation of the array theories developed in this paper through flow visualization. Acoustic enhancement was also accomplished through low frequency white noise excitation of the hairpin vortex array.

# A Flow Visualization Study of Acoustically Enhanced Hairpin Vortices

by

Stephen A. Whyte

A thesis submitted in partial fulfillment of the

requirements for the degree of

Master of Science in Aeronautics and Astronautics

University of Washington



1993



Approved By _____
(Chairperson of the Supervisory Committee)

Program Authorized
to Offer Degree Aeronautics and Astronautics

Date December 8, 1993

In presenting this thesis in partial fulfillment of the requirements for a Master's degree at the University of Washington, I agree that the Library shall make its copies freely available for inspection. I further agree that extensive copying of this thesis is allowable only for scholarly purposes, consistent with "fair use" as prescribed in the United States Copyright Law. Any other reproduction for any purposes or by any means shall not by allowed without my written permission.

Signature 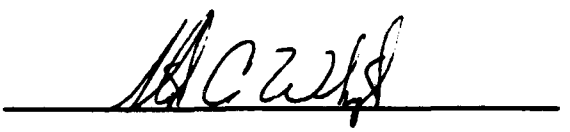

Date December 8, 1993

**University of Washington**

Abstract

A Flow Visualization Study of Acoustically
Enhanced Hairpin Vortices
by Stephen A. Whyte

Chairperson of the Supervisory Committee:
Professor Mitsuru Kurosaka
Department of Aeronautics and Astronautics

For many years the turbulent boundary layer was thought to be composed of totally chaotic and random eddies. However, recent work has shown that a very organized array of structures exist in this regime. These structures, named hairpin, horseshoe or Λ- shaped vortices, compose a major portion of the turbulent boundary layer and may be responsible for the increased heat transfer seen in turbulent regimes.

The hairpin vortex is a vortex line that has been lifted off of the surface and through mutual induction of its legs forms a loop. This loop is composed of two counter-rotating legs, oriented at 45 degrees to the wall, with a head that joins the two legs together. These legs act like tornados sweeping along the wall. They transport air adjacent to the wall up through the legs and into the head. Research at the University of Washington has shown that this 'tornado effect' increased the heat flux away from the wall. If this capability can be harnessed and enhanced, the effects of film cooling in turbine engines can be dramatically increased.

Earlier research at the U of W has demonstrated the effects of a single hairpin; however, the effect of the hairpin array are not understood. This thesis presents new theories into hairpin array growth with the goal of acoustic enhancement of the array structure. Research in a turbulent boundary layer has given initial confirmation of the array theories developed in this paper through flow visualization. Acoustic enhancement was also accomplished through low frequency white noise excitation of the hairpin vortex array.

## TABLE OF CONTENTS

## LIST OF FIGURES

## LIST OF TABLES

## LIST OF NOMENCLATURE

| Variable | Description |
|---|---|
| $\delta(x,U,\upsilon)$ | Boundary layer thickness |
| $\delta^*(x,U,\upsilon)$ | Displacement thickness |
| $\upsilon$ | Kinematic Viscosity |
| a | Speed of sound |
| d | Significant length |
| f | Frequency |
| L | Cross-sectional length |
| $N_{array}$ | Number of hairpin vortices passing a given cross-section, x , per unit of time, or the array rate |
| $N_{2D}$ | Number of hairpin vortices passing a given point in the cross section, x, per unit of time, or the 2-D rate |
| f'(x,y) | Number of hairpin births per unit area of the flat plate per unit time |
| $f_{shed}(x,y)$ | Frequency at which hairpin vortices are created per unit area of the flat plate per unit time |
| p' | Pressure |
| S(f,v,d) | Strouhal number |
| t | Time |
| u' | Normal velocity |
| $U_\infty$ | Freestream velocity |
| V | Velocity |
| v' | Tangential velocity |
| x | Distance from leading edge of test plate |
| X | Unit length in x |
| y | Cross-sectional distance |
| Y | Unit length in y |

# ACKNOWLEDGMENTS

The author wishes to express sincere appreciation to those individuals who helped make this research effort a success. My family was always there for support and guidance without which I would never have reached this level of success in life. Jennifer, you have been my support and encouragement throughout my time in Seattle. Professor Mitsuru Kurosaka, thank you for your assistance and counsel in preparing this thesis. Thanks to Mr. Robert Blair whose long hours of dedicated assistance made this research possible. And finally, to the Zoomies who always reminded me that college life was meant to have plenty of good times and great friends.

## DEDICATION

To the two most important people in my life:

my DAD:

"illigitimi non carburundum";

and

Jennny Lynn:

"with one word you changed my life forever"

# INTRODUCTION

## Background

The turbulent boundary layer is one of the most non-understood topics in aerodynamics. For many years it was accepted that the turbulent boundary layer was composed of purely random and chaotic events. In recent times, however, this view has changed. Researchers, such as Perry, Lim and Teh[1] and Head and Bandyopadhyay[2], have determined that specific orderly structures do exist in turbulent boundary layers. These structures have become known by many names, the most common of which are hairpin, horseshoe or Λ-shaped vortices. The current theory of turbulent boundary layers maintains that the boundary layer is composed of an array of organized hairpin structures. The vortices appear to form when the span-wise vorticity is lifted off of the surface by a normal velocity component or a surface protrusion. Once a section of the vortex line is lifted off of the surface, the mutual induction of the vortex causes the head to elevate further and the legs to come together. The elevation continues until an equilibrium condition is reached. This occurs when the hairpin reaches the point of least shear, at about a 45 degree angle to the wall. The growth of the vortex continues until it leaves the region of shear, the boundary layer.[3] At this point the head of the hairpin curls over which inhibits further growth. This growth process is depicted in Figure 1.1.

Two aspects of this model are not yet understood. Is there a pattern to this seemingly random vortex array, and does this array add to the heat transfer away from the wall? The second question is a topic of further investigation and will not be discussed as part of this thesis.

The pattern of the hairpin array would seem to be dependent upon its components and their characteristics. The formation of one hairpin would appear to cause the formation of another. The counter rotating legs cause an updraft between them. The normal component of this updraft would seem to lead to the formation of another hairpin. However, this has not been experimentally determined to be the case. Is it rather that the hairpins are formed based upon a natural frequency that has yet to

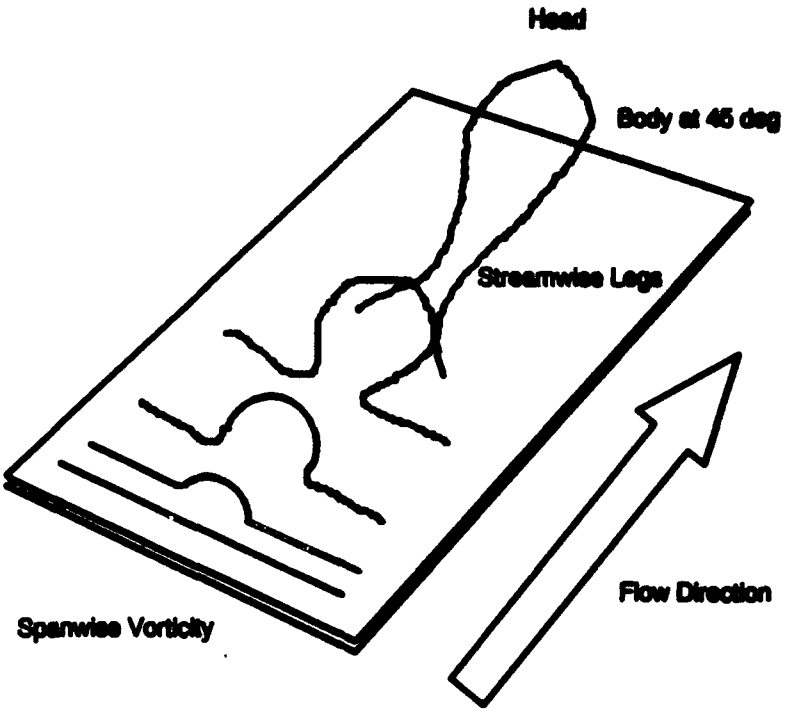


**Figure 1.1**: Depiction of natural hairpin growth

be determined? And does that frequency determine the shedding rate of the hairpins? That is the topic of this research, to attempt to determine the natural frequency and the natural shedding frequency of the hairpin vortices, and to relate that frequency to a Strouhal number based upon the displacement thickness of the boundary layer. Furthermore, the knowledge of these frequencies should allow the use of acoustic excitation to enhance the vortices.

## Theory

### *Hairpin Vortex Structure*

The hairpin vortex is a very complex structure. The vortex is composed of two counter-rotating legs connected by a head with the legs oriented along the axis of least shear, or at a 45 degree angle to the wall. If we assume the vortex has constant circulation and is in solid body rotation, it can be shown the rotational velocity inside the vortex is equal to the flow velocity outside the vortex.[4] This means that the legs

act as tornados sweeping along the surface of the plate. The pressure gradient due to the changing velocity causes the flow along the wall to be drawn up through the legs into the head. This feature is referred to as corewise transport or the tornado effect. The added fluid transport causes the vortex to grow until it extends outside the area of shear, or boundary layer. At this point the head turns, inhibiting further growth of the vortex.

The main features of this structure, from a streamwise viewing are the head that should contain a large amount of injected fluid, and legs that are inclined at 45 degrees to the wall. A crossflow viewing will show either a vortex loop or counter rotating legs depending upon the illumination angle. A visual depiction of the key features of these views are shown in Figure 1.2.

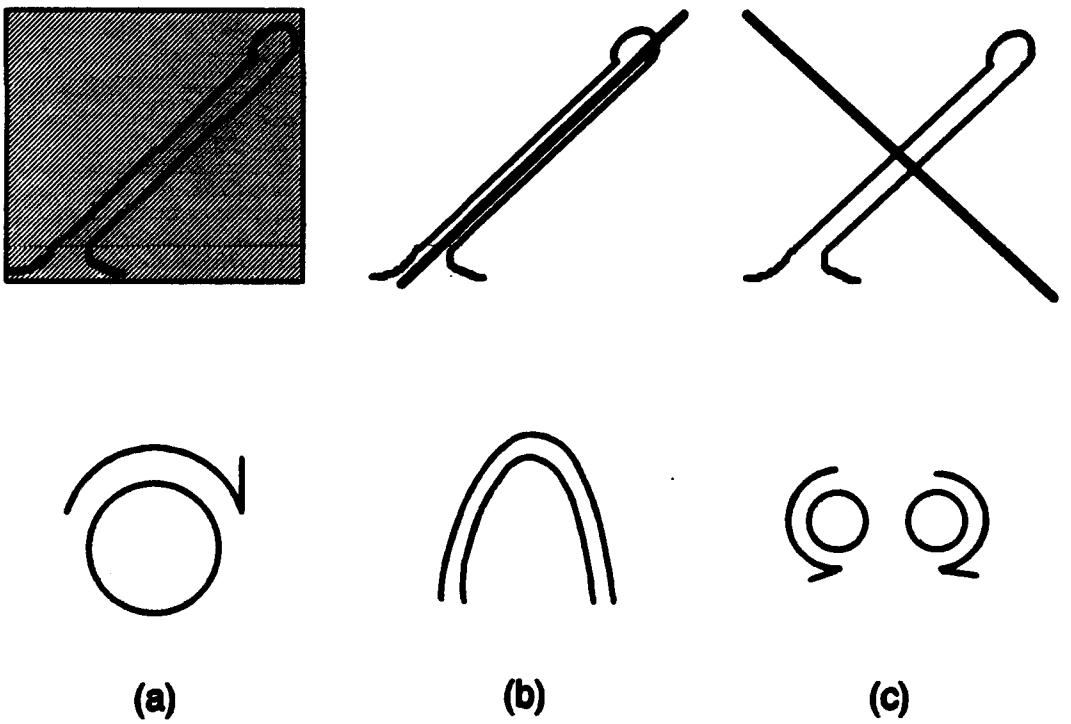


**Figure 1.2**: Visual depiction of the key features of a hairpin vortex based upon illumination angle: a) streamwise, b) 45 degrees upstream, c) 45 degrees downstream.

***Hairpin Array Structure***

The vortex array should also show some interesting features. Vortices have a certain natural shedding frequency at which they are formed, and in some cases also have a natural frequency at which they are found. These two frequencies can be different depending upon whether the vortices are created or destroyed over time. The non-dimensional number that describes this behavior is called the Strouhal number and is defined in (1.1) where f is the frequency, d is a significant length dimension and V

$$S = \frac{f * d}{V} \tag{1.1}$$

is a velocity. For this project f will be a natural frequency, d is expected to be the boundary layer displacement thickness, $\delta^*$, and V will be the freestream velocity. Research has shown that the Strouhal number is constant for most vortices. If this is assumed to be true, then the frequency can be written as (1.2).

$$f = \frac{S * U_\infty}{\delta^*} \tag{1.2}$$

As the flow moves spatially down a flat plate the boundary layer thickness, $\delta$, and displacement thickness growth, $\delta^*$, are defined by (1.3).

$$\delta = \frac{0.37 * x}{\left(\frac{U_\infty * x}{\upsilon}\right)^{\frac{1}{5}}} \qquad \delta^* = \frac{\delta}{8} \tag{1.3}$$

These equations show that as x, the distance downstream from the leading edge of the

plate, increases the displacement thickness increases. This in turn means that if the Strouhal number and freestream velocity are constant, the frequency is constantly decreasing. This does not agree with the known information about hairpin vortices.[5] This research has found no mechanism for vortex destruction but rather has shown that more hairpin structures constantly created. Also, it does not seem likely that they are combining. For an example we will look at an array of 2-D vortex lines. This array is a fairly stable structure. As one line is displaced the mutual induction of the two adjacent lines tends to return it to a stable position. Therefore, this simple 2-D analogy suggests that this mutual induction is not a mechanism for creation or destruction of larger vortex structures.

Based upon this research, it seems that the frequency calculated from the Strouhal number does decrease. But intuitively, we expect the frequency to increase as more hairpins are being formed. For that reason this frequency can not be the number of hairpin that exist at any one point in time or the natural frequency of the array. Therefore, a new model is needed. The frequency calculated from the Strouhal number however, could be the number of hairpins created at any location and time or the natural shedding frequency. This would mean that the number of vortices is constantly growing as more hairpins are created.

If we revisit the 2-D vortex line analogy again we can see that as the number of vortex lines increases, the spacing must decrease. This can continue to happen until a minimum spacing is reached. After this point the filaments are pushed so close together that either no further growth is achievable or full scale destruction of the array occurs. Therefore, we should expect a maximum value of hairpins to be reached as more and more vortices are created.

This gives us a good model but is difficult to test because the creation process is difficult to find visually. Therefore, it would be helpful to know the actual number of hairpins passing a cross-section, x, per unit time or the array rate, $N_{array}$. In order to find this rate, we should be able to integrate the number of new hairpin vortex births per unit area of the flat plate from the leading edge of the plate to the desired x location and across the cross sectional dimension of the plate. The rate of births will

be defined in (1.4) where X is the unit length in x and Y is the unit length in y.

$$f'(x,y) = \frac{f_{shed}(x,y)}{(X)(Y)} \tag{1.4}$$

If all of the new births are assumed to survive the growth process then the array passing rate is shown in (1.5).

$$\begin{aligned} N_{array} &= \int_0^x \int_0^L f'(x,y)\, dx\, dy \\ N_{array} &= \int_0^x \int_0^L \frac{f_{shed}(x,y)}{(X)\,(Y)}\, dx\, dy \end{aligned} \tag{1.5}$$

If the shedding frequency is assumed to be independent of y as it is defined in (1.2) then the result is (1.6).

$$N_{array} = \frac{L}{Y} \int_0^x \frac{f_{shed}(x)}{X} dx \tag{1.6}$$

By substitution and integration the result is shown in (1.7), where x is the location where the array rate is desired.

$$N_{array} = 108.1 * \left(\frac{S * U_\infty^{\frac{9}{5}}}{\upsilon^{\frac{1}{5}}}\right) * x^{\frac{1}{5}} \tag{1.7}$$

This is the rate of hairpin passage for the entire cross section of the flow at that x location. In order to determine the number of hairpins in a streamwise sheet, this value must be divided by the number of hairpins that occur across that section, or in other words, the horizontal spacing must be known. A value for this spacing was proposed by Head and Bandyopadhyay in 1981. The spacing they determined was $100\upsilon/U_\tau$. However, this value was determined at one x location with a constant cross-section dimension. The model presented here would indicate that the spacing

should scale with both the distance downstream and the cross-sectional width. For this reason the number of hairpins passing a point in the cross-section, x, per unit time, or the 2-D rate, will be used as defined in (1.8), where n is the number of hairpins that occur across the cross section at that location.

$$N_{2D} = \frac{N_{array}}{n} = 108.1 * \left(\frac{S * U_{\infty}^{\frac{6}{5}}}{n * \upsilon^{\frac{1}{5}}}\right) * x^{\frac{1}{5}} \qquad (1.8)$$

According to this equation the array rate, or the number of hairpins at any location and time, should increase with increased x position or velocity. In other words, as the x position and velocity are increased, the 2-D rate should increase and the horizontal spacing between hairpins should decrease. The 2-D rate is also measurable by flow visualization and with the measurement of the horizontal spacing the array rate can be calculated.

This new model does present some interesting ideas that seem to explain much of what is known, however many questions remain to be answered. First, does a constant Strouhal number exist for the array formation? If true, then the array rate would approach infinity as x approaches infinity. This does not seem possible based upon knowing some minimum spacing must exist. This would indicate either the Strouhal number is dependant on x at some location so that a constant number of hairpins will be formed and further growth will be retarded, a condition of static equilibrium, or a constant Strouhal number exists and array destruction occurs once the minimum spacing between hairpins is exceeded and then the hairpin growth cycle begins again out of the chaos and a condition of dynamic equilibrium is reached.

A closer look at law of entropy may give a better understanding. It seems that as more and more hairpins are formed, a more organized structure to the turbulent boundary layer is formed, a nice clean array of hairpin vortices rather than the chaotic state that is expected. This would seem to defy entropy. However, if instead of

looking at the movement of air particles, we look at the vorticity, a new understanding could be reached. If the vorticity at transition is assumed to be an array of vortex lines, equally spaced with equal strength, a very organized structure is present. As hairpin vortices are created from the twisting of these lines, the organized structure becomes more chaotic. This would indicate that the result would be a random array of vorticity, with no organized structure. This would seem to indicate that as more and more hairpins are created, the vorticity field becomes more random until when the minimum spacing is reached the hairpins interact that destroy the array. This would create a chaotic vorticity field that would not allow for further hairpins to be created directly from the chaos. But the vortex lines created from the flow over the plate at any location would seem to wrap up into new hairpins that would eventually destroy the organized vorticity field at some location downstream.

In order to verify this model, several questions must be answered:

1) Does a constant Strouhal number exist that is independent of x?
2) If the Strouhal number is constant, is the dimensional scaling $\delta^*$ as expected?
3) Does the cross sectional dimension influence the array frequency?
4) Will these hairpins be influenced by acoustic excitation like other vortices; what effect will enhancement create, and at what frequencies will this enhancement occur?
5) What happens at small values of x to the Tollmien-Schlichting wave as shown by Perry, Lim, and Teh[6]. Does the wave type structure develop into hairpin structures downstream and become part of the hairpin array? Would this increased initial population cause the hairpin array to reach a maximum value at an earlier x location compared to the normal array growth rates described in this paper?
6) What happens after the maximum population is reached? Does the formation of new hairpins stop (static equilibrium), or does a full scale destruction occur and the process repeats itself until the next maximum is reached (dynamic equilibrium).

7) How does the law of entropy apply to this problem? (a restatement of 6 since a static equilibrium would seem to defy entropy)
8) How will the hairpin array with its corewise transport influence heat transfer away from the wall?

This new model, if experimentally upheld, should lead to a better understanding of the hairpin vortex itself and the array of the structures. This project will attempt to answer the first four questions raised and attempt to shed some light onto the other areas. The other questions are items of future study and their implications will be discussed as part of the Future Items of Interest section of this thesis.

## Experimental Facility

All experiments were conducted at the University of Washington's Aerodynamic Laboratory. This facility was renovated during 1992 to include an Engineering Laboratory Design Incorporated three foot by three foot low speed, low turbulence wind tunnel. The drive unit is a 200 Hp constant speed, variable pitch three phase motor with 16 blades. The tunnel configuration and position in the building are shown in Figure 1.3.

### *Facility Modifications*

Several modifications were made to the initial building layout for this project. These changes are noted by the shaded regions in Figure 1.3.

The main reason for the modifications were made as a result of the high sound pressure levels. When the building was modified in order to accommodate this particular wind tunnel the result was an open area 100 feet long, 20 feet wide, and 20 feet high. The bottom 10 feet in height was constructed of solid concrete with wood

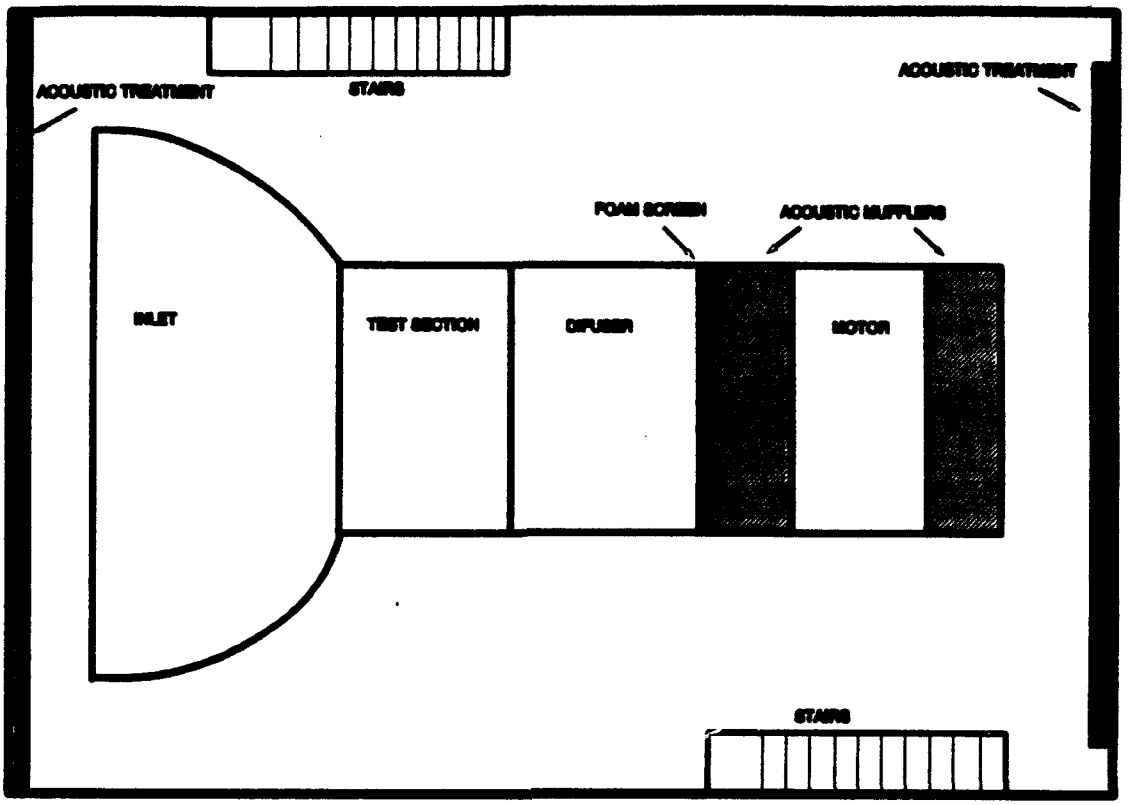


**Figure 1.3**: Schematic of the University of Washington's Aerodynamics Laboratory

and windows making up the upper half. This created the problem of acoustic propagation of the tunnel created sound.

Tests were completed using a Brüel and Kjaer high resolution signal analyzer. These tests showed a broad band decibel level of 120 dB plus certain pure tones above that level inside the test section. An analysis of these frequencies showed that the largest contributors were the electrical frequencies (60 Hz and its higher order modes) and the blade passing frequency (480 Hz and its higher order modes). Due to the sound level being above human discomfort levels a serious effort was put into decreasing the levels of sound intensity for both the broad band and the pure tone frequencies. In order to decrease the sound intensity, several steps were taken to alter the acoustic behavior.

Acoustic silencers were placed upstream and downstream of the motor section in order to absorb sound closest to the source. These sections are the diameter of the

tunnel at that location and are built of sound absorbent material. Also, sound absorbent foam was installed on the front and back walls. This step created a major improvement because it stopped the sound propagation off of the walls and back into the room. These steps provided a drop in the acoustic levels in the room down to about 70 dB broad band and 80 dB pure tone. However, the test section levels were still substantially higher than desired.

The sound levels in the test section were not the only problems with running this experiment. The variable pitch system used to create air flow required the blades to be twisted in order to run at relatively low speeds. For this project, I was interested at running near 5 m/s, under the original threshold for the tunnel. In order to solve both of these problems, three inches of foam were placed between the test section and the fan. This increased drag caused the fan to run at a higher angle of attack for a given speed. The result was a tunnel that could run in the 2-7 m/s range. The foam also proved to be an effective sound absorber. The result was good airflow in the desired range with a broad band acoustic level of 70 dB and a maximum pure tone of 85 dB.

This foam screen is a simple modification that can be installed and removed by crawling through the test section and the diffuser and securely placing the three inches of foam against the screen already in place at that location. The foam sections used are cut over size so that a secure, compressed fit is accomplished. The only point of caution is to ensure that the tunnel is not allowed to run with a reversed flow field, a positive angle of attack on the blades is always needed.

### *Test Section Modifications*

The test section in the wind tunnel is three feet by three feet and eight and one half feet long made of clear acrylic. In order to create a boundary layer that started at a known point a test plate was installed one foot from the top with the lower surface used for testing. A schematic of the overall configuration is shown in Figure 1.4.

The use of the lower surface would allow for all buoyancy forces to be

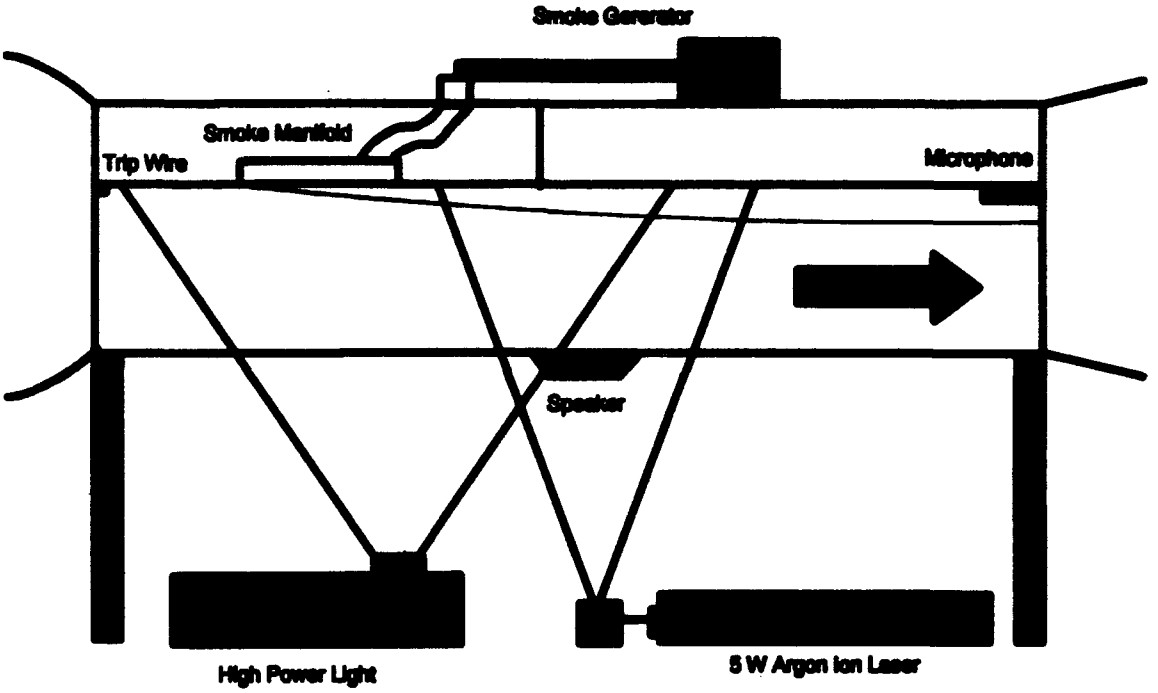


**Figure 1.4**: Schematic of the test section configuration.

neglected. A 0.003 inch nichrome wire was installed at the leading edge in order to trip the flow. A 0.03 inch slot was also placed in the plate at two locations to allow for smoke injection into the boundary layer The slots were placed at 6 inches from the leading edge and at one quarter chord of the plate (~ .75 m).

The smoke generation system was created by Shojiro Shindo and Otto Brask at the University of Washington.[7] The smoke is allowed to flow into a manifold where the pressure gradient along the surface of the plate is able to suction the smoke into the boundary layer. A schematic of the injection technique is in Figure 1.5.

Two illumination schemes were used for the flow visualization. A laser was used in order to visualize the cross section of the boundary layer at different locations and angles. A 5 watt Argon Ion laser was necessary to provide sufficient illumination of the smoke particles. The other scheme was a 2000 watt Xenon light scurce that would illuminate the entire upper surface of the boundary layer.

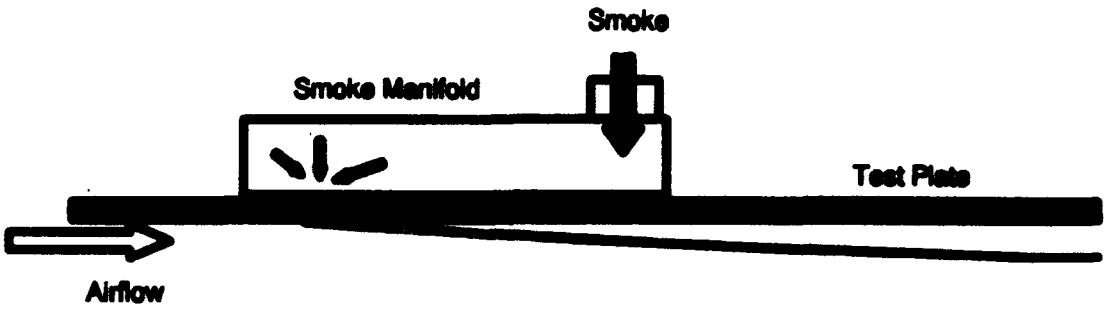


**Figure 1.5**: Schematic of the smoke injection system.

The optics scheme for the laser was quite simple. The laser housing was installed on the floor of the building downstream of the test section pointing toward the test section. A vibrating mirror was used to create the sheet of light. A streamwise sheet of light made by placing the vibrating mirror directly in the path of the laser beam. For a crosswise sheet of light, a first surface mirror was used to turn the beam 90 degree and then the vibrating mirror was placed in the beam. For the angled crosswise beams, the vibrating mirror was inclined at the necessary angle. A schematic of this is shown in Figure 1.6.

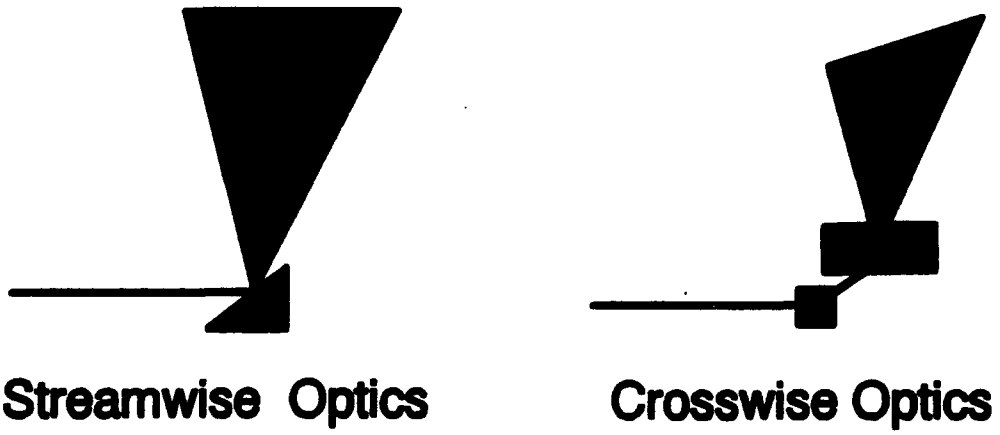


**Figure 1.6**: Schematic of optical system.

The acoustic excitation system was created with a very simple system. A signal generator was used to produce the desired signal. This signal was then passed through an amplifier to a set of speakers. This set of speakers could be driven in phase or out of phase depending upon the polarity of the connections. This allowed

for greater ability to create the resonance modes needed for excitation of the boundary layer structures. The frequency of the signal was determined using calibrated condenser microphone and a Brüel and Kjaer high resolution signal analyzer.

The flow visualization was viewed with a SVHS camera with a shutter speed of 1/500 s. A Wratten No. 57A filter was used in some applications in order to cut down the background light and allow for better visualization of the subject matter. The frame speed was restricted to 60 frames per second as with all video systems.

**Initial Tests**

An initial set of tests were accomplished to ensure accurate flow in the test section with all of the modifications. The first test was devised to test for possible separation at the leading edge. A smoke probe was placed upstream of the plate to visualize the flow around the leading edge. These tests showed a large separation bubble with turbulent reattachment. It was determined that the large amount of blockage on the upper side of the plate caused a downward trend to the streamlines and hence separation. In order to solve this problem the plate was inclined to a 0.5 degree angle of attack and a small amount of blockage was added to the lower section of the plate behind the test section. The result was attached flow around the leading edge with only very small changes to the pressure gradient.

The second test was conceived to test the effectiveness of the trip wire. Hot wire measurements were conducted at 2.00 m downstream from the leading edge with and without the trip wire. The resulting boundary layer profiles are shown in Figure 1.7. The shape parameter for these curves is 1.58 where 1.4 is theoretically turbulent and 3.0 is laminar and therefore is assumed to be turbulent with the main difference being the boundary layer thickness. This difference can be attributed to the trip wire causing turbulent growth from the leading edge while without it, the boundary layer must transition from laminar to turbulent.

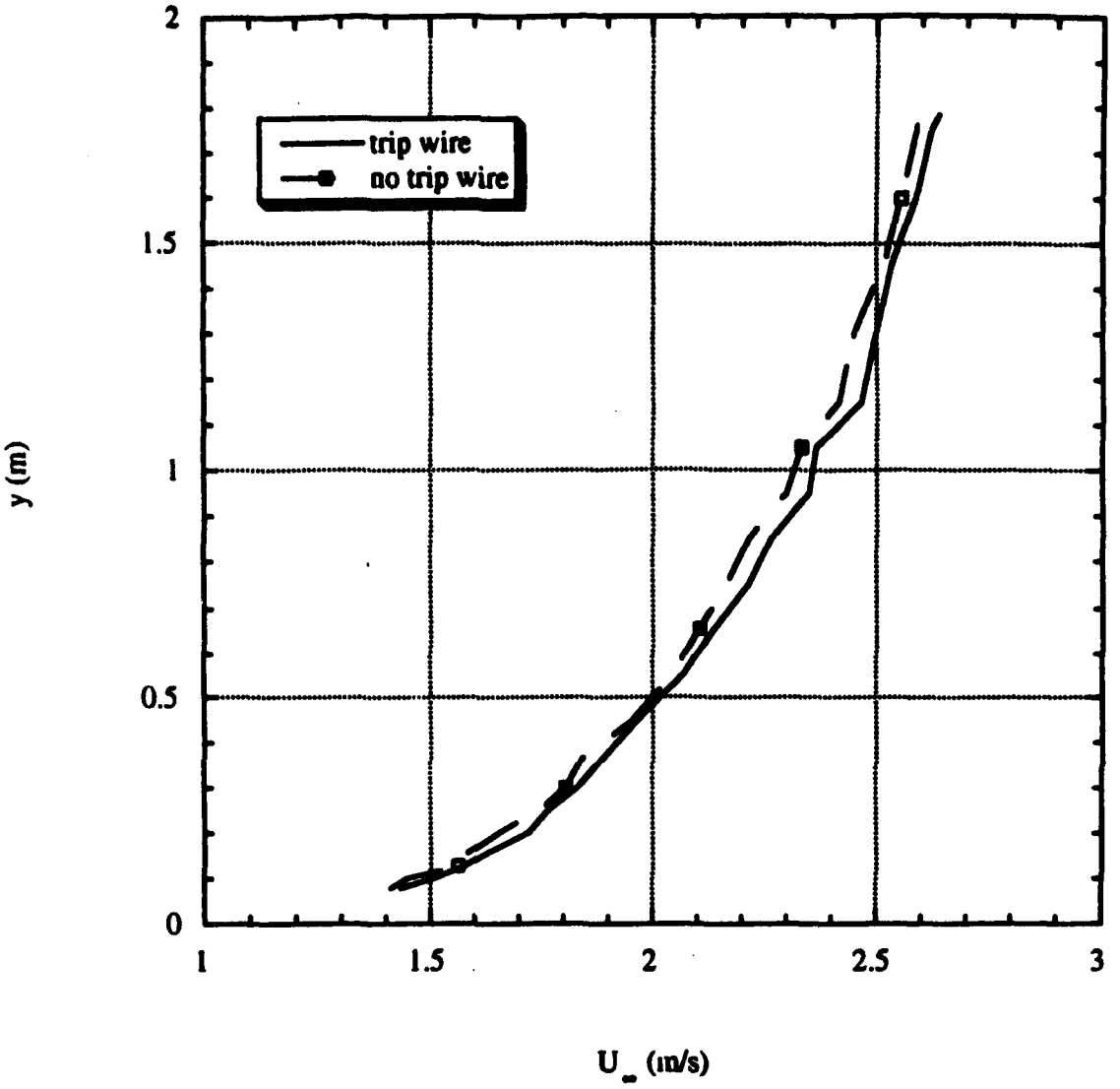


**Figure 1.7: Boundary Layer Profiles with a trip wire and without a trip wire.**

## HAIRPIN IDENTIFICATION

### Experimental Procedure

The purpose of this set of tests was to visually identify the hairpin vortices. The only conclusive visual evidence of hairpins in turbulent boundary layers was conducted by Head and Bandyopadhyay in 1981[8]. They were able to determine the particular features in a turbulent boundary layer that correspond to the hairpin structures. However, one main difference exists between their experiment and our setup. Head and Bandyopadhyay were able to view the boundary layer an additional two and one half meters downstream. Therefore, for a first step a repetition of their experiment was conducted.

The experimental setup was kept as shown in Figure 1.4. The first step was to view a laser sheet in the streamwise direction. This view would show the progression of hairpins moving down stream with the flow. This view would also give an indication of the number of hairpins present in the boundary layer and the 2-D rate.

Two other views were chosen to give a three dimensional picture of the vortex structure. These views are at 45 degrees upstream and 45 degrees downstream. A visual representation of these angles are shown in Figure 2.1. These views should show the horizontal spacing of the structures as well as the overall shape of the vortex.

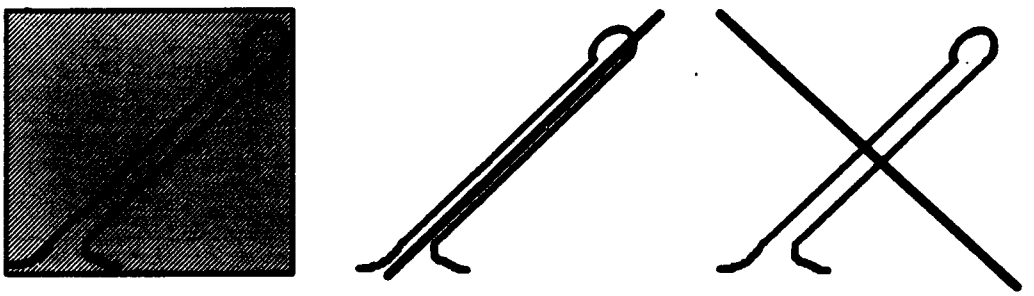

**Figure 2.1**: Sketch showing light plane illumination angles: a)streamwise, b)45 degrees upstream, c)45 degrees downstream.

The velocity and location of the sheets were varied in order to get a

macroscopic understanding of the growth of the vortex array. Velocities tested were 3 m/s, 4 m/s, and 5 m/s. The locations were at 1.0 m and 2.0 m from the leading edge.

A step by step experimental procedure is included in Appendix B. This procedure should allow for these experiments to be repeated at a future point in time.

## Results

### *Streamwise Visualization*

The first step in this experiment was to determine the existence of hairpin vortices in the turbulent boundary layer. This process was accomplished by looking at a streamwise sheet of illuminated smoke particles. Sample frames of this view at two locations for three different velocities are included in Figure 2.2. One of the key features of these frames are the definite 45 degree slopes in the flow. This is a very strong indication of the presence of hairpin vortices. In a normal turbulent boundary layer, one without hairpin vortices, we would expect a random distribution of the smoke particles. But instead, the smoke appears to be grouped into structures and these structures are inclined at a 45 degree angle to the wall.

The next strong indication of the presence of hairpin vortices are the bright pools of smoke that appear to be islands above the boundary layer. This would indicate hairpins because the tornado effect would cause the head to contain a strong concentration of smoke particles. As the hairpin grows, the head would rise out of the boundary layer and take with it the smoke particles. The legs would appear as swirling smoke. Since one streamwise cross section can not cut both the head and the legs, the swirling smoke that appears at the 45 degree angle is the smoke entrained by the legs as they rotate in the smoke filed boundary layer.

Once the hairpin structures were identified, they could be counted. By viewing 60 consecutive frames (one second of time) and counting every occurrence of a hairpin structure, the approximate 2-D rate could be determined. It was found that the

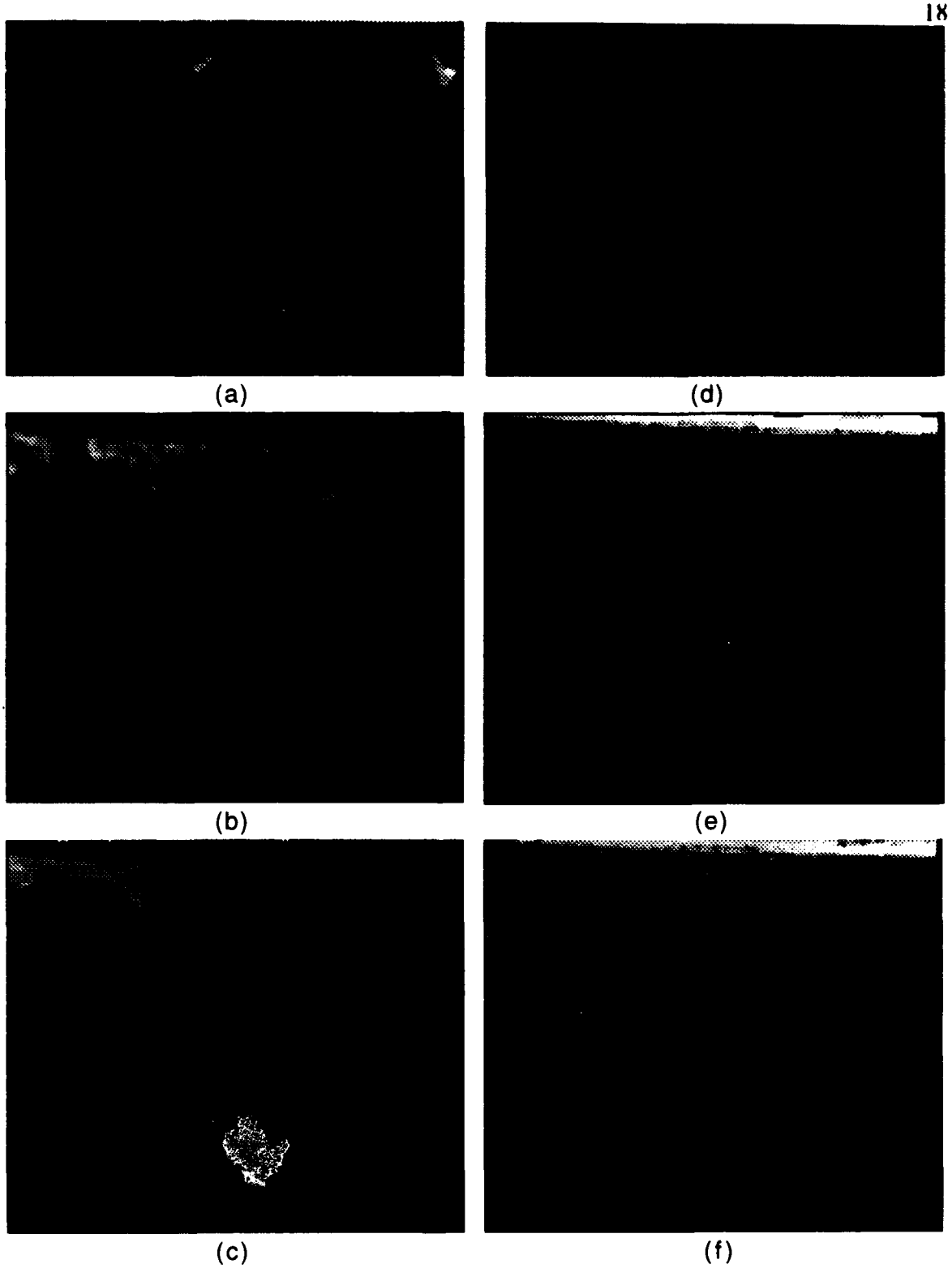


**Figure 2.2**: Streamwise view at the indicated velocity and x position from the leading edge: a) 3.0 m/s at 1.0 m, b) 4.0 m/s at 1.0 m, c) 5.0 m/s at 1.0 m, d) 3.0 m/s at 2.0 m, e) 4.0 m/s at 2.0 m, and f) 5.0 m/s at 2.0 m

hairpins did not occur at regular intervals. They would occur in groups of different sizes at irregular intervals. This measurement was conducted numerous times at two locations until an average 2-D rate was found. The results of this study are shown in Table 2.1.

**Table 2.1**: Summary of 2-D rates for varying velocities and x positions.

| $U_\infty$ (m/s) | x (m) | $N_{2D}$ (1/sec) |
|---|---|---|
| 3.0 | 1.0 | 20 |
| 4.0 | 1.0 | 21 |
| 5.0 | 1.0 | 22 |
| 3.0 | 2.0 | 20 |
| 4.0 | 2.0 | 22 |
| 5.0 | 2.0 | 23 |

The expectations that the array frequency would increase with x position downstream and with increased velocity are upheld by this study but not quite to the level expected by theory. This would indicate that the Strouhal number must calculate the shedding frequency and not the array frequency.

***Upstream View***

The upstream view cuts the hairpin vortex along it long axis as shown in Figure 2.1. This view will show the entire vortex loop, but more importantly will be able to show the spacing between the vortex loops. This will provide more information on the vortex array structure and development process.

The turbulent boundary layer was cut by a laser sheet at approximately 45 degrees to the wall. Sample frames are shown in Figure 2.3 for varying velocities and

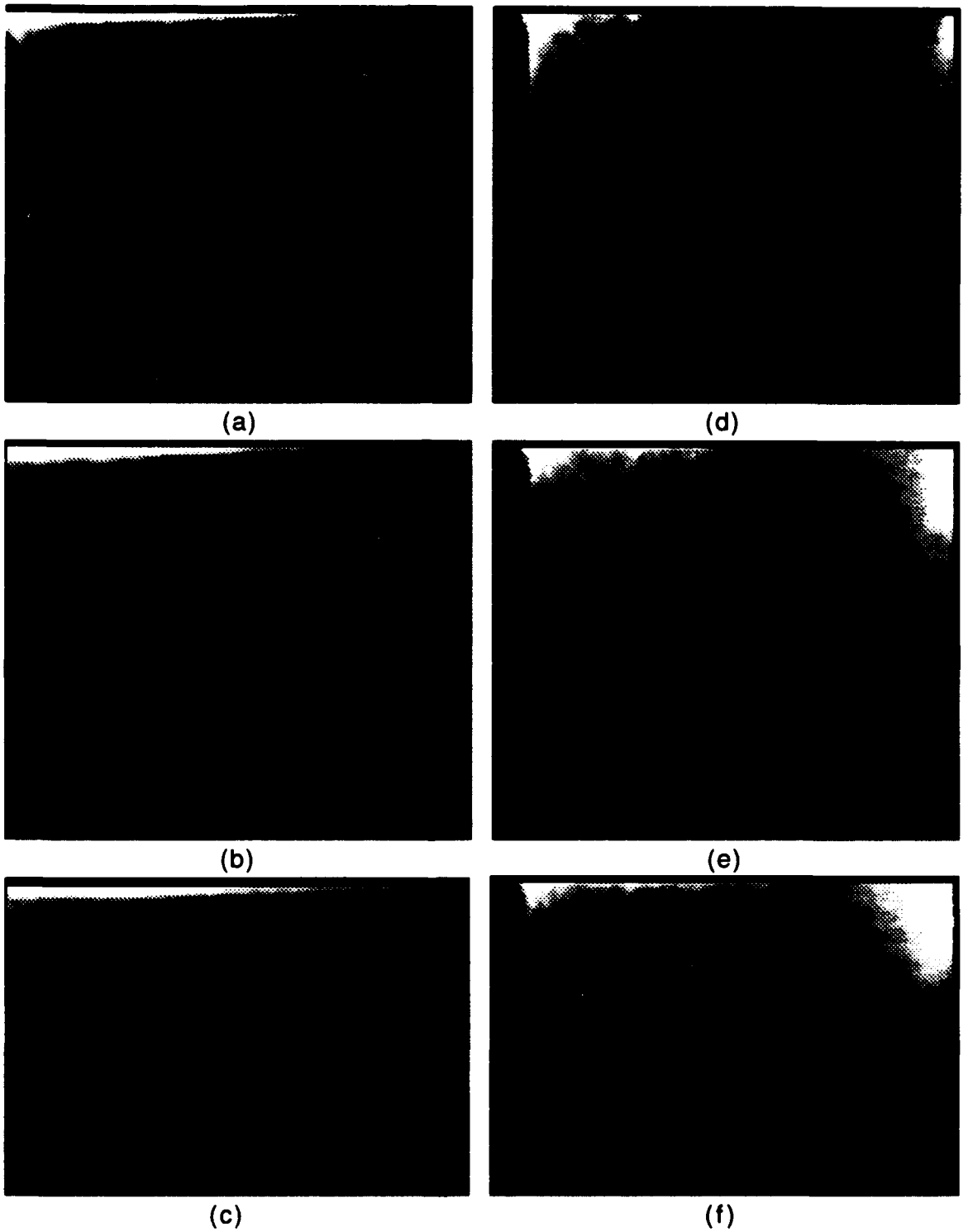


**Figure 2.3**: Upstream view at the indicated velocities and x position: a) 3.0 m/s at 1.0 m, b) 4.0 m/s at 1.0 m, c) 5.0 m/s at 1.0 m, d) 3.0 m/s at 2.0 m, e) 4.0 m/s at 2.0 m, and f) 5.0 m/s at 2.0 m.

x positions.

These views show the vortex loops that were expected in this view. The spacing between structures was measured as the distance between the center of adjacent vortex loops. The spacing distances for these cases are tabulated in Table 2.2.

**Table 2.2**: Summary of spacing between hairpin vortices depending upon velocity and x position.

| $U_\infty$ (m/s) | x (m) | Spacing (m) |
|---|---|---|
| 3.0 | 1.0 | 0.075 |
| 4.0 | 1.0 | 0.056 |
| 5.0 | 1.0 | 0.044 |
| 3.0 | 2.0 | 0.068 |
| 4.0 | 2.0 | 0.050 |
| 5.0 | 2.0 | 0.038 |

It can be seen that the spacing distance does decrease with increased x position and velocity as we would expect. As the flow moves downstream, more and more hairpin structures are added to the flow and the spacing must decrease.

***Downstream Angle***

The downstream angle is the third angle investigated. This angle dissects the vortex along its short axis and is designed to view the counter rotating legs. This allows us to get an understanding of the inner structure of the vortex loop. The counter rotating legs will not only draw fluid from the wall with the tornado effect but will also entrain fluid along its outer boundary. This accounts for only a very small percentage of the hairpin composition but is important because this entrainment causes

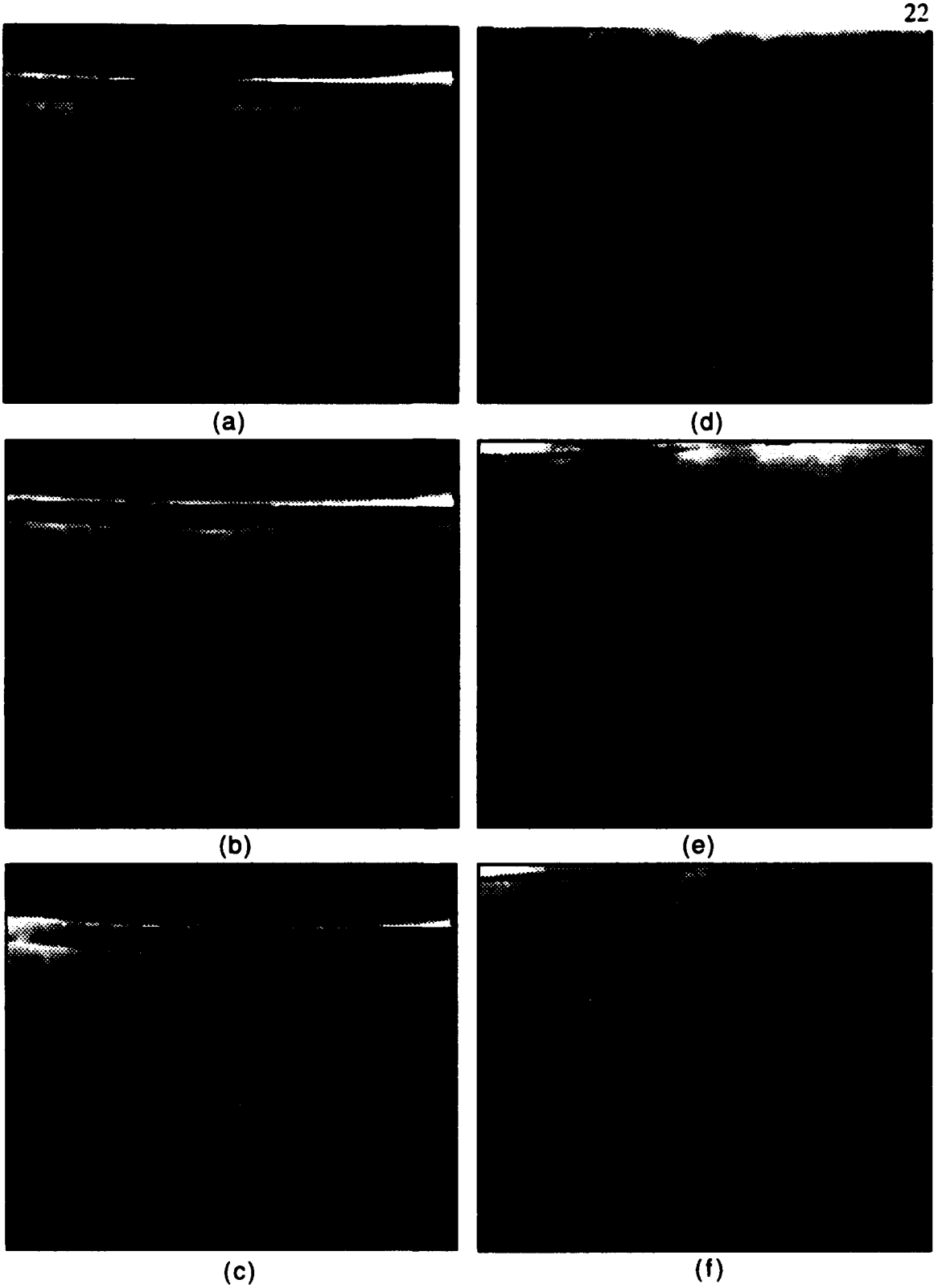


**Figure 2.4**: Downstream view at the indicated velocities and x position: a) 3.0 m/s at 0.75 m, b) 3.0 m/s at 2.0 m, c) 4.0 m/s at 0.75 m, d) 4.0 m/s at 2.0 m, e) 5.0 m/s at 0.75 m, and f) 5.0 m/s at 2.0 m.

the updraft between the legs that may be the cause of new hairpin development.

The boundary layer was viewed at three different velocities and at two different x locations. Sample frames of this view are seen in Figure 2.4.

These frames show that the legs are indeed counter rotating and do entrain fluid along their outer boundary. This causes an updraft between the legs and a down draft outboard of the legs.

Measurements of the spacing between hairpin structures appear to be very similar to the measurements given in the previous section and display the same trends.

**Summary**

These visualization tests show that hairpin structures are a definite part of the turbulent boundary layer. The streamwise views show that as the x position increases the number of hairpins also increase. This indicates that more hairpins are constantly created. The cross-sectional views indicate that the structures are hairpins with vortex loops and counter rotating legs. The spacing of the structures does decrease with x position and increased velocity.

Once the 2D rates and spacing was determined the information could be used to calculate the Strouhal number. If (1.7) is solved for the Strouhal number, the result is (2.1).

$$S = \frac{f * \upsilon^{\frac{1}{3}}}{108.1 * U_{\infty}^{\frac{6}{5}} * x^{\frac{1}{5}}} \qquad (2.1)$$

If the 2D rate and the spacing are combined together, an array rate can be determined from (1.8). Table 2.3 is a summary of the array rates and the corresponding Strouhal number for that case. It can be seen that the Strouhal numbers seem to be nearly constant over this range of velocities and x positions. The approximate Strouhal seems to be 0.07.

**Table 2.3**: Calculation of Strouhal numbers based upon 2D rates and spacing of naturally occurring hairpin vortices.

| $U_\infty$ (m/s) | x (m) | $N_{2D}$(1/s) | space (m) | $N_{array}$(1/s) | S |
|---|---|---|---|---|---|
| 3.0 | 1.0 | 20 | 0.075 | 267 | 0.071 |
| 4.0 | 1.0 | 21 | 0.056 | 375 | 0.071 |
| 5.0 | 1.0 | 22 | 0.044 | 500 | 0.072 |
| 3.0 | 2.0 | 20 | 0.068 | 394 | 0.069 |
| 4.0 | 2.0 | 22 | 0.050 | 440 | 0.072 |
| 5.0 | 2.0 | 23 | 0.038 | 605 | 0.076 |

## PRESSURE IDENTIFICATION

### Experimental Procedure

Once the hairpins structures were identified visually and an approximate array frequency was identified, a test was needed to determine the exact frequency. These tests were conceived for that purpose.

Hot-wire measurements are very well adapted to determining the turbulence levels and frequencies of small scale variations. However, they do not respond well to large scale structures. Therefore, another technique was needed. Mike Fox at the University of Washington discovered that condenser microphones were able to sense the pressure fluctuations caused by large scale structures and determine the frequency of those fluctuations. It is felt that this is due to the fact that a microphone can pick up the passing of more than one structure. It can also sense the passing of a structure adjacent to its position.

These tests used a variation of those methods. A condenser microphone was placed in the flow, oriented parallel to the flow and along the wall of the test plate. This configuration allowed the microphone to sense the pressure fluctuations of the hairpin vortices as they passed that position.

The microphone signal was transmitted through a pre-amplifier to a Brüel and Kjaer high resolution signal analyzer. The resulting frequency plot was analyzed to determine any large frequency variations that may indicate a hairpin passing frequency. This analysis was accomplished at varying velocities and x locations.

The result would be an indication of the frequency dependance on location and velocity, or the actual Strouhal number. As the velocity or position was changed the frequency spectrum would change. A shift in a frequency spike would indicate a change in the frequency of the hairpin vortices. It is expected that the Strouhal number will remain constant regardless of velocity or position changes.

A step by step experimental method is included in Appendix B.

**Results**

The first set of tests conducted were for a constant x location with varying velocity. Five sets of tests were conducted for velocities 3.0 m/s to 6.0 m/s at an x location of 2.0 meters downstream. Several tests were performed for each test case. A sample frequency spectrum for each test case is provided in Figure 3.1.

It can be seen certain frequencies display higher sound pressure levels than others. Each plot contains certain frequency spikes. The Strouhal numbers for each of the spikes indicated with arrows are tabulated in Table 3.1. The table shows that a constant Strouhal number does seem to exist for a varying velocity range. This means that a linear relationship exists between velocity and the frequency.

**Table 3.1**: Summary of pressure data for constant x position (x = 2.0 m).

| $U_\infty$ (m/s) | x (m) | $\delta^*$ (m) | f (Hz) | S |
|---|---|---|---|---|
| 3.0 | 2.0 | 0.0070 | 28 | 0.065 |
| 3.5 | 2.0 | 0.0068 | 37 | 0.072 |
| 4.0 | 2.0 | 0.0066 | 44 | 0.073 |
| 4.5 | 2.0 | 0.0064 | 48 | 0.068 |
| 5.0 | 2.0 | 0.0063 | 53 | 0.072 |

The flow visualization measurements showed that a definite frequency pattern did not exist for the overall scale of the flow. The fluctuations are more random and have a single frequency for only small time blocks and then it changes. Even a small time change, when averaged over a few seconds, will cause many spikes rather than a single definite indication of the frequency. The indicated noise spikes are there, but are not repeatable in every test. This leads to the notion that the shedding frequency is at the frequency indicated, but since the shedding at any one location will only produce a few hairpins at that frequency and crosswise location, signal will be

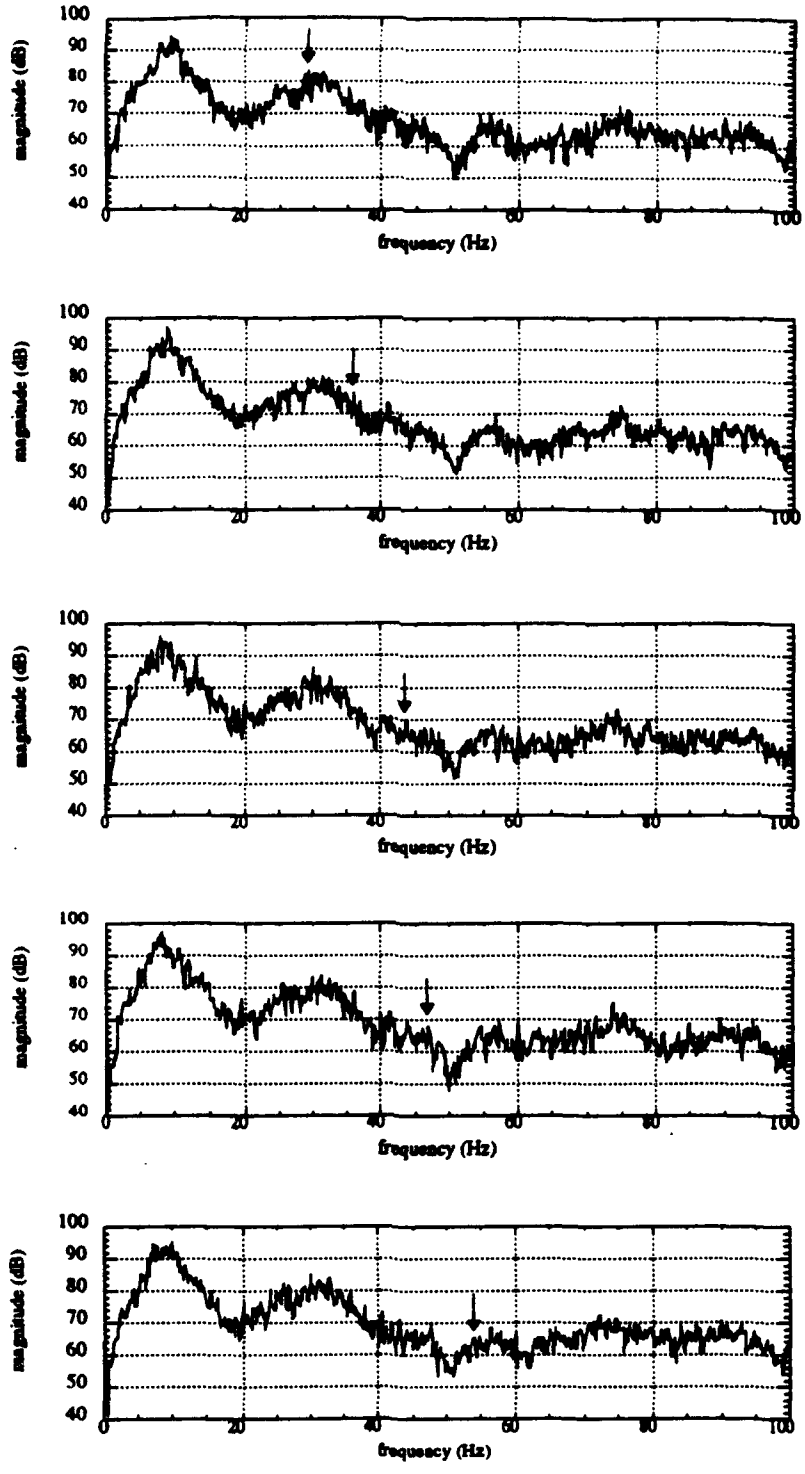


**Figure 3.1**: Frequency spectrum of airflow over the plate at x=2.0 with a velocity of: a) 3.0 m/s, b) 3.5 m/s, c) 4.0 m/s, d) 4.5 m/s, e) 5.0 m/s.

intermittent. This data shows that to be true.

The next step was to verify a constant Strouhal number for varying x location. This was accomplished at constant velocity by moving the microphone to different locations. The frequency spectrum plots for these cases are shown in Figure 3.2.

Again certain frequencies display higher sound pressure levels. These spikes are marked with arrows and are tabulated in Table 3.2. A correlation between plots indicate that a type of inverse relationship exists. By the approximate correlation to a constant Strouhal number appears to be an x to the minus four fifths relationship. This indicates that as the x position increases the frequency decreases. Based on information from the last chapter, this would indicate that the frequency sensed by the microphone is the shedding frequency of hairpin vortices.

**Table 3.2**: Summary of pressure data for constant velocity ($U_\infty$ = 4.0 m/s).

| $U_\infty$ (m/s) | x (m) | $\delta^*$ (m) | f (Hz) | S |
|---|---|---|---|---|
| 4.0 | 0.5 | 0.0022 | 129 | 0.071 |
| 4.0 | 1.0 | 0.0038 | 72 | 0.068 |
| 4.0 | 1.5 | 0.0052 | 53 | 0.069 |
| 4.0 | 2.0 | 0.0066 | 42 | 0.069 |
| 4.0 | 2.5 | 0.0079 | 35 | 0.069 |

The two sets of tests appear to show a constant Strouhal number between 0.065 and 0.075. This data is consistent with the hairpin studies conducted in laminar boundary layers. Acarlar and Smith in their studies with synthetic hairpins showed a Strouhal number between 0.05 and 2.0 depending upon the injection velocity and slot size.[9] Perry, Lim and Teh determined a Strouhal number of 0.1 for their studies of Tollmien-Schlichting waves.[10] A difference does exist between turbulent and laminar boundary layers, but this difference may have nothing to do with the mechanism for the creation or destruction of the hairpin structures. It would seem that the comparison

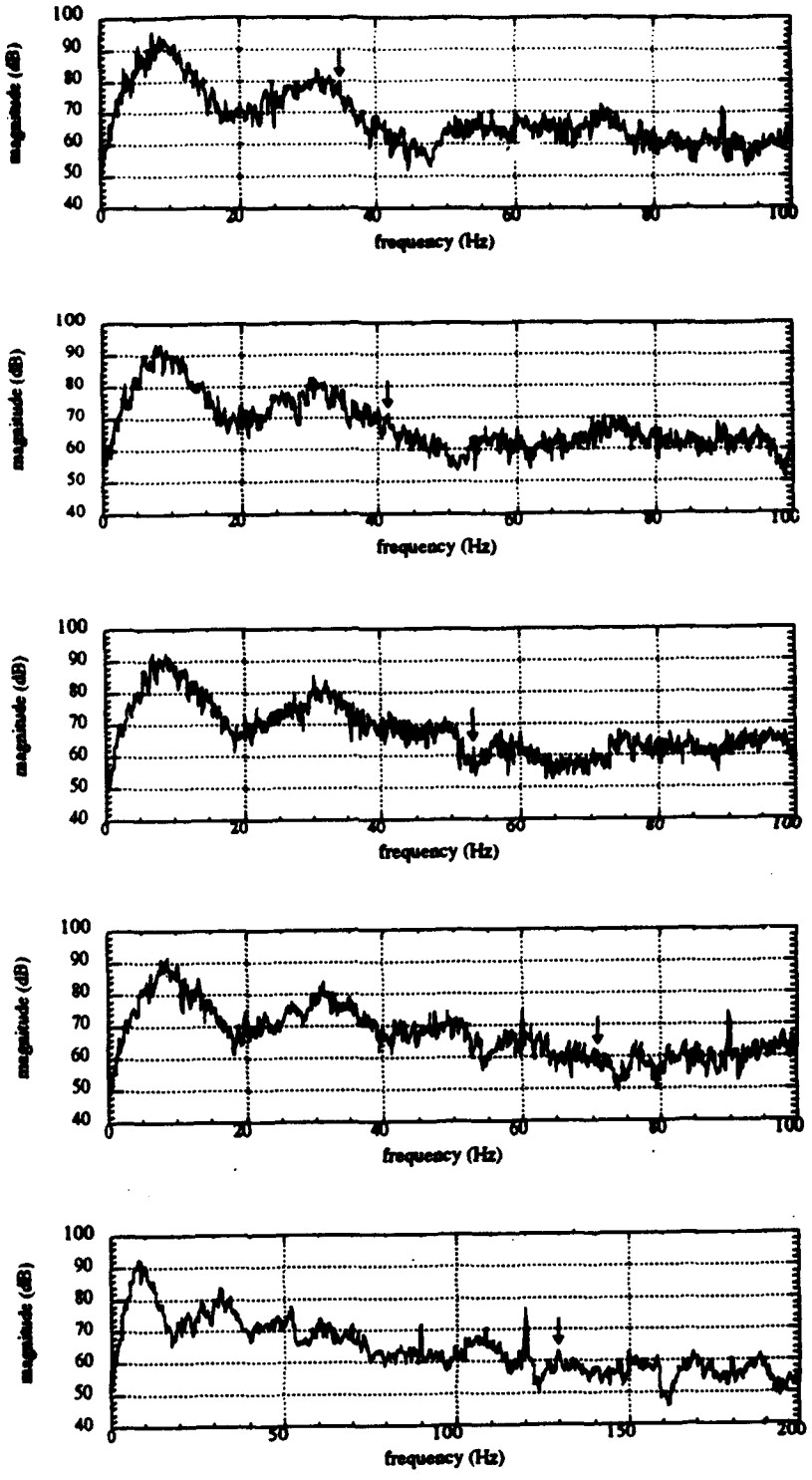


**Figure 3.2**: Frequency spectrum of airflow over the plate at V = 4.0 m/s with an x position of: a) 2.5 m, b) 2.0 m, c) 1.5 m, d) 1.0 m, e) 0.5 m.

between the Strouhal numbers indicates this is true.

## Summary

This set of pressure tests indicates that a constant Strouhal number exists for varying velocities and x positions. This Strouhal number is in the range of 0.06 to 0.08. This range may be a function of a non constant displacement thickness or velocity. Also, the decreasing frequency with increasing x location indicates that the frequency spikes correlate to the shedding frequency of the hairpin vortices.

## ACOUSTIC ENHANCEMENT

### Experimental Procedure

The purpose of this set of tests was to enhance the hairpin vortex structure with the use of acoustic waves. Vortices of all types become enhanced through growth or greater definition. This is important because a larger, more defined structure is easier to understand and to use in application.

The first reason for enhancement is to understand the vortex structure. Research has been accomplished in laminar flow that has identified the hairpin structure; bu is this structure the same in a turbulent regime? Data collected up to this point seems to point to that conclusion, but larger and better defined structures may give more light to that comparison.

The second reason deals with the corewise transport issues of the vortex structure. If the vortex becomes larger and more defined, it should result in more fluid being entrained into the structure either through the tornado effect or outer entrainment. This will cause a greater percentage of smoke in the vortex and it should appear more defined. Future studies would then look at the heat transfer applications of increased corewise transport.

In the case of the hairpin structure, enhancement may have only small visual effects. The vortex growth is confined to a certain size based upon the boundary layer thickness. This would seem to indicate that more fluid would be entrained early and the initial growth would be rapid. Once it grew to the size of the boundary layer, growth would stop. The structure should be more clearly defined visually because it would entrain a greater percentage of smoke into the upper regions of the vortex loop. But this research will not be able to determine if the increased corewise transport will continue even if the growth is constrained. That question will have to be answered by future research. For this research, only the increased definition and increased smoke particles in the upper regions of the vortex results will be investigated.

The frequency at which this enhancement occurs is expected to be the natural shedding frequency because that is the only frequency that would have an effect on the

early stages of vertex formation. This frequency is calculated based upon the Strouhal number defined in (1.2). This will be accomplished in two stages. First, an attempt at looking at the pure tone response will be accomplished. This will only look at the enhancement of vortices created at one location. This would seem to enhance only a few vortices per second and so will be hard to gage the effectiveness. The second and more easily determined will be an attempt at enhancing the vortices in the broadband. This will be accomplished by introducing a white noise signal in the desired frequency regime.

A step by step experimental procedure is provided in Appendix B.

**Results**

The first step was to establish the frequency at which a pure tone signal would create enhancement at a given location. The previous research indicated a Strouhal number of approximately 0.07. This would indicate the ranges of frequency given in Table 4.1.

**Table 4.1**: Frequency ranges predicted for acoustic enhancement.

| $U_\infty$ (m/s) | x range (m) | frequency range (Hz) |
|---|---|---|
| 3.0 | 0.5 - 2.0 | 91 - 30 |
| 4.0 | 0.5 - 2.0 | 130 - 43 |
| 5.0 | 0.5 - 2.0 | 169 - 56 |

In order to test these predictions, a pure tone signal was generated in these ranges and the results viewed. The results were inconclusive. It appeared that one or two vortices per second were more defined. But because the growth was restricted by the boundary layer it was difficult to determine if the enhancement was enhancement

and not just random increases in the corewise transport.

Based upon this result, the broadband experiment was conducted. Even thought the results were for the most part inconclusive, there was enough data to suggest that the white noise should be limited to the ranges specified in Table 4.1. For that reason a band-pass filter of 3-100 Hz with a roll off of 3 dB per octave was used. This would allow for a large amount of energy in the range of 15 - 200 Hz to be added to the flow. 15 Hz was the low frequency limit on the speaker employed. This setup created an increase of 10 dB in the Sound Pressure Levels for the range of interest.

Flow visualization studies were completed for velocities of 3.0 m/s and 4.0 m/s at x locations of 1.0 m and 2.0 m. The results are presented with a side by side comparison of naturally occurring and acoustically treated hairpins for the three angles (streamwise, upstream and downstream) in Figure 4.1 through Figure 4.4.

These figures show that the enhancement does not increase the hairpin size as expected but it does seem to increase the corewise transport. The amount of smoke particles, judged by the brightness of the hairpin, seems to be larger in the enhanced frames. This is especially true in the upper regions of the vortices. This would seem to indicate that the acoustic enhancement principles do apply at least to the corewise transport. This research does not indicate if the growth is faster or if the increased corewise transport continues once the vortex has grown to full size. Also this does give more evidence that the Strouhal number for the shedding of hairpins is on the order of 0.07.

**Summary**

The acoustic enhancement of the hairpins create more defined hairpins with a larger proportion of smoke particles than the non-enhanced, especially in the upper regions of the vortices. This indicates that acoustic waves at the right frequencies create increased corewise transport in hairpins. The overall growth remained unchanged but enhancement may lead to faster development or longer periods of

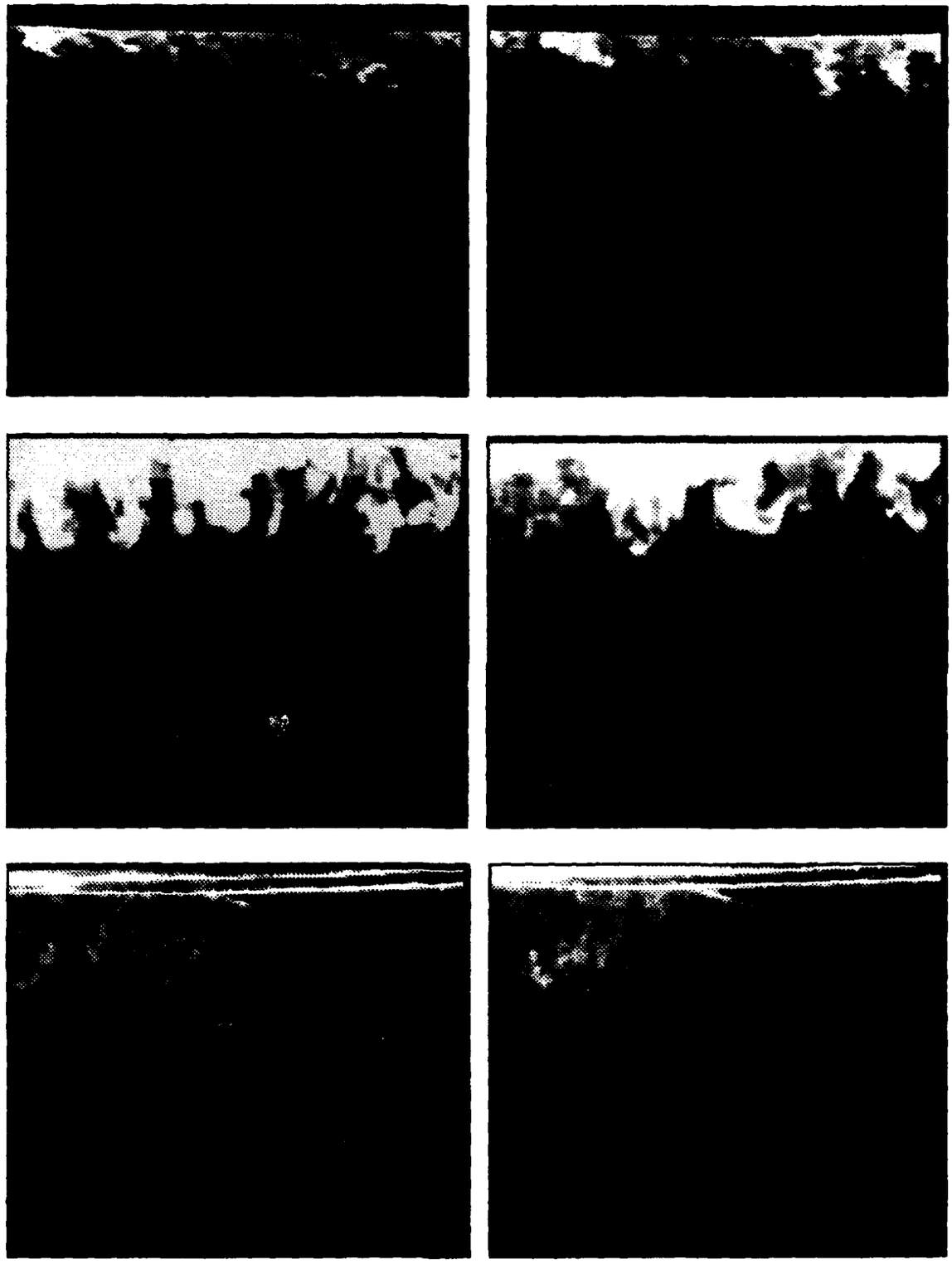

**Figure 4.1**: Side by side comparison of natural to acoustic enhancement for x = 1.0 m and V = 3.0 m/s.

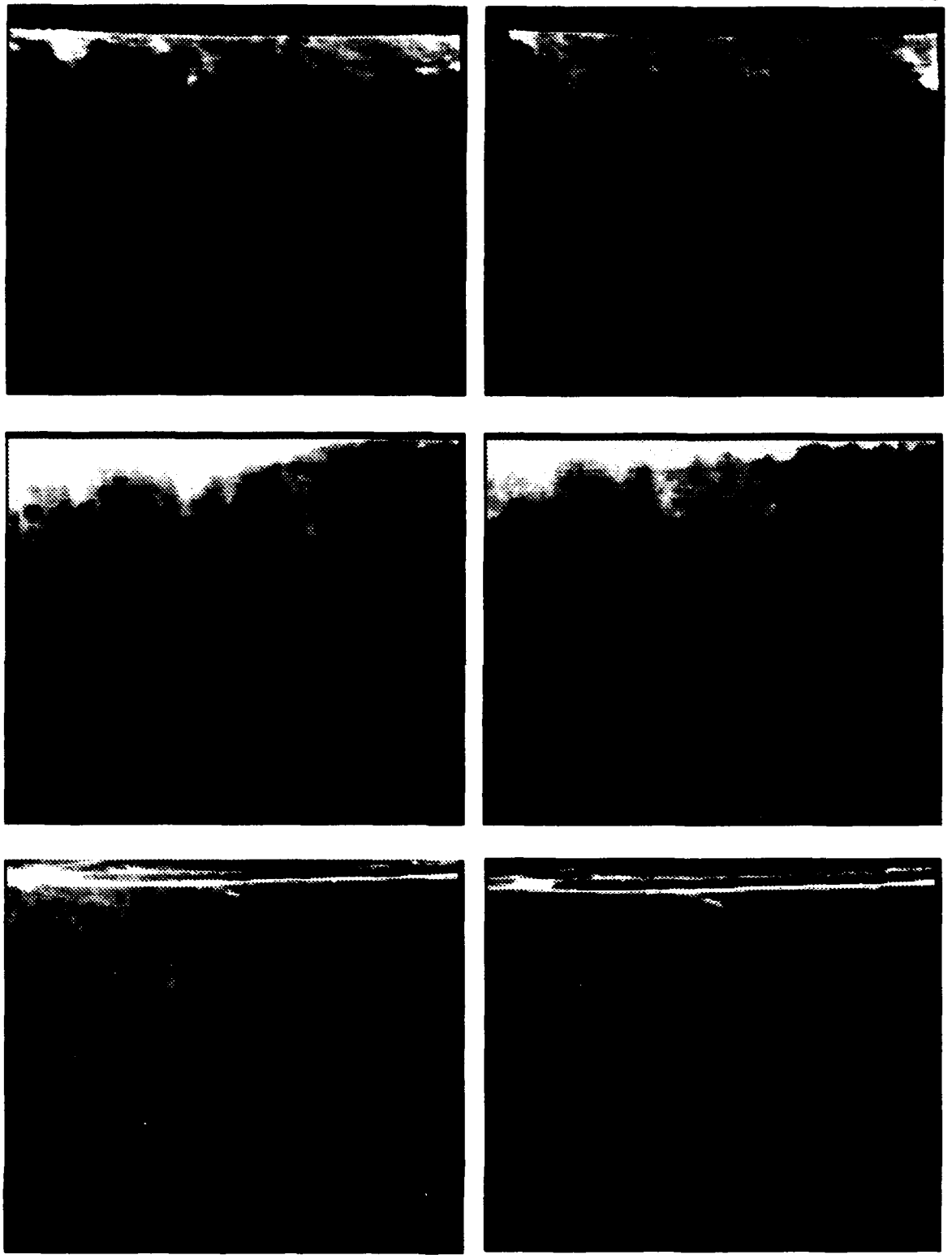

**Figure 4.2**: Side by side comparison of natural to acoustic enhancement for x = 1.0 m and V = 4.0 m/s.

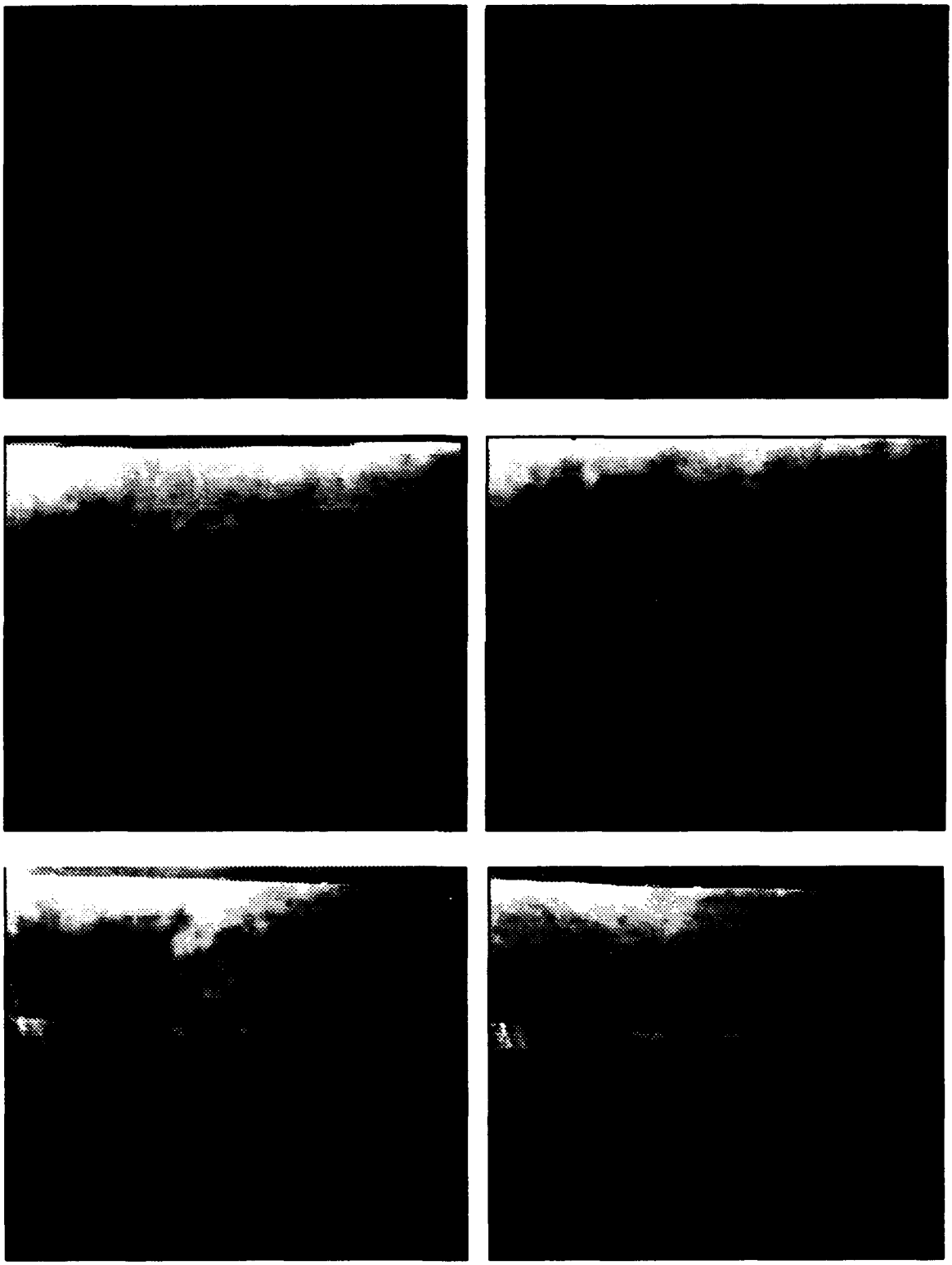

**Figure 4.3**: Side by side comparison of natural to acoustic enhancement for x = 2.0 m and V = 3.0 m/s.

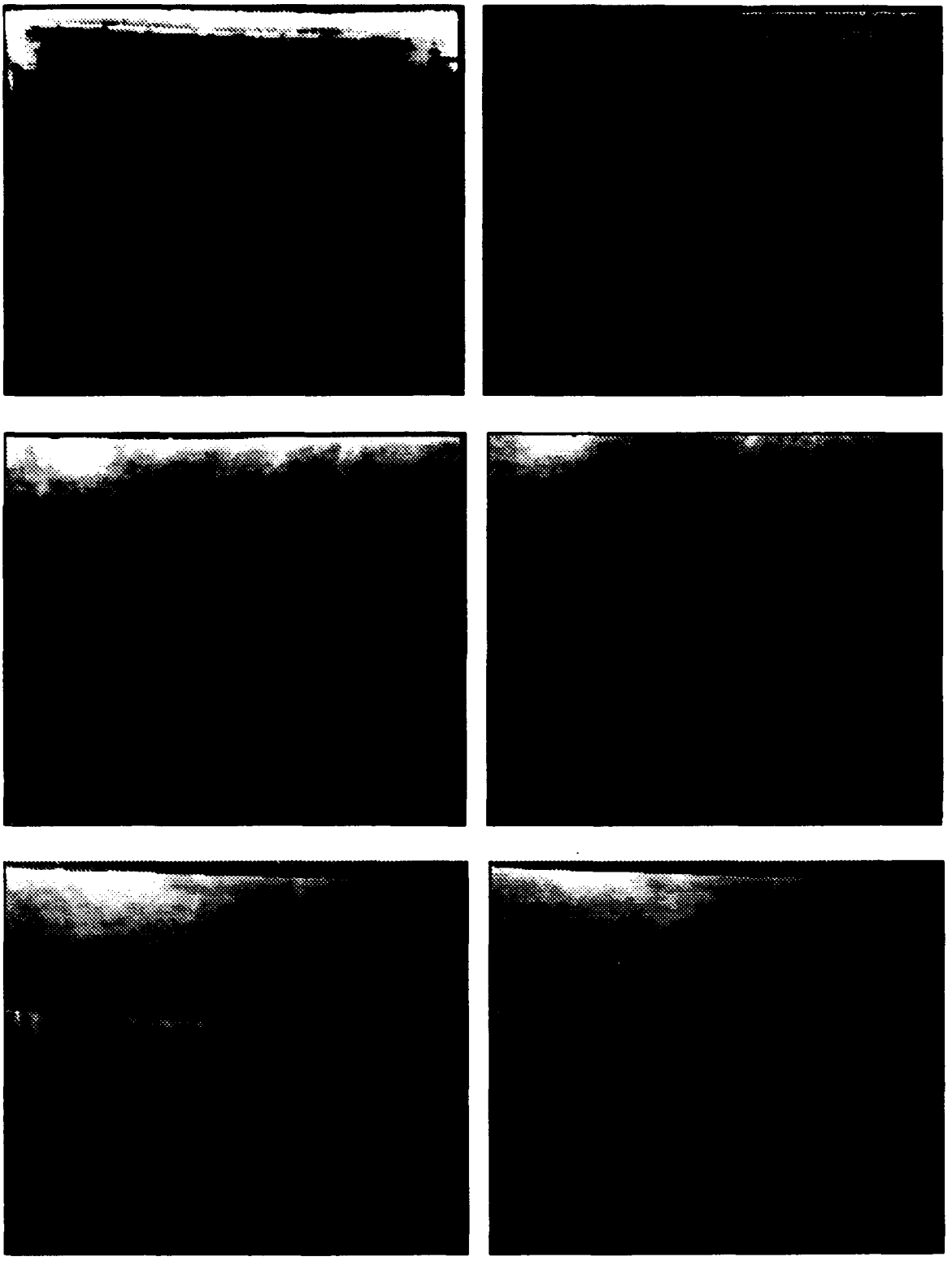

**Figure 4.4**: Side by side comparison of natural to acoustic enhancement for x = 2.0 m and V = 4.0 m/s.

corewise transport (two topics of further interest). It also appears that white noise is more desirable because of the broad scale effects. It is still to be determined if a right frequency will be able to excite all of the hairpins at one time.

## CONCLUDING REMARKS

The research presented in this thesis is a part of a research project to understand the mechanics of and applications for hairpin vortices. This research is the first look into the hairpins that occur as part of the turbulent boundary layer. As such it was designed to only answer some questions derived from the project's laminar counterpart. But in the research effort, this project created more questions than it answered.

Therefore, the study evolved into a preliminary look into the creation process of the array structure. The formation process of one hairpin vortex is understood but the array structure is far from that point. In this presentation of the conclusion I will first present the results obtained, and then present other areas and questions that still must be answered.

### Conclusions

This research appears to validate the model of hairpin vortex array structures presented in the theory section of this thesis. The array seems to grow in number as the flow moves downstream, but the growth rate is slower as x increases. This supports the idea that the shedding frequency decreases with increasing x position as the Strouhal number would indicate.

The flow visualization study determined of the 2-D rates of passage and the crosswise spacing of the hairpins. It was found that with increasing x position and velocity the 2-D rates increased and the cross sectional spacing decreased. This allowed for the array passing rate to be calculated and then the Strouhal number to be solved for the varying x locations and velocities. This showed a constant Strouhal number based on the displacement thickness of approximately 0.07 This shows that a constant Strouhal number exists independent of x (at least for up to 2 meters) and that the dimensional scaling of the displacement thickness is correct as expected. Also it was found that the array rate is very intermittent on a time scale less than one second.

A second result of this study is that the cross sectional dimension should

influence the maximum array rate. If the cross sectional dimension is reduced the same amount of vortices will be created but must fit into a tighter space and the spacing will decrease until the minimum spacing is reached and dynamic or static equilibrium will be reached. This result would indicate that if the cross section was reduced, the equilibrium number would be reduced for static stability and the time between occurrences of the maximum number of hairpins will be reduced for dynamic equilibrium.

The pressure measurements indicate this to be true again and shows that the vortex array is not steady. The frequency analysis of the pressure data displays an intermittent signal that appears to contain frequency spikes that correspond to a Strouhal number of 0.07. This data is a validation of the previous study.

The next step was to determine the effect of acoustic excitation. It was determined that the hairpin vortex is changed by acoustic waves. This influence increases the amount of corewise transport but can not change the size of the vortex because that is a function of the boundary layer thickness. This increased corewise transport, however, may increase the growth rate of the vortex until it reaches maturity. But nonetheless the increased corewise transport did increase the amount of smoke particles in the vortex, especially the upper regions. It was found that a pure tone signal seems to influence the vortices created at one location, but in order to enhance the overall array, a white noise signal was needed. This frequency of excitation seemed to agree very well with a Strouhal number of 0.07 but this is inconclusive because the growth process of vortices at one location could not be tracked.

The vortex array structure seems to be dependant on the vorticity field created by flow over the flat plate. The hairpins are a mechanism that uses the organized field in order to do work, corewise transport, and in that process creates a random vorticity field that no longer can perform work. But, the flow over the plate creates more vorticity than in turn creates more vortices. This seems to be a dynamic problem that starts over once the maximum array frequency is reached. In order to use these structures for useful corewise transport, like increased heat transfer, the location of the

maximum array frequency and the strength of the vortices at that location are items of research that must be accomplished.

**Future Research**

The research also added a lot of insight into future research that would allow a more significant insight into the vortex array formation and appearance.

In order to solve the remaining problems several steps may help. A water tunnel study should lead to some insight into the array formation process. First, the slow speed should increase the ability to track each hairpin and determine how that hairpin is responsible for the formation of others. The next step is to determine the type of equilibrium (static or dynamic) that the array possess. It appears that the array is going to be dynamic and so changes in the cross sectional dimension and use of a Tollmien-Schlichting wave to increase initial population may help to determine the periods between maximum populations, the maximum array rates and if the destruction of one array helps in the formation of another array.

The final step would be to look at the heat transfer away from the plate. The heat transfer would appear to be directly influenced by the distance downstream. The heat transfer should increase as more hairpins are forming, reach a maximum when the maximum array frequency is reached and then drop off significantly only to rise again in a dynamic fashion.

## ENDNOTES

1. Perry, Lim, and Teh, 1981.
2. Head and Bandyopadhyay, 1981.
3. Head and Bandyopadhyay, 1981, pg 331
4. Jeff Hagen, 1992, pp. 4-6.
5. Head and Bandyopadhyay, 1981.
6. Perry, Lim and Teh, 1981.
7. Shindo and Brask, 1969.
8. Head and Bandyopadhyay, 1981.
9. Acarlar and Smith, 1987, Part 2, p. 55.
10. Perry, Lim, and Teh, 1981, pp. 382.

# APPENDIX A: ACOUSTIC BEHAVIOR

Vortices have proven to emit a particular frequency. For instance, the wind past an electric line will appear to sing. This is caused by the shedding frequency of the Karman Vortex Street arising from the airflow past a circular cylinder. Also it has been shown that vortices can be enhanced if they are excited by a periodic disturbance at its natural frequency. This is the case with both vibrating wires and acoustic waves. The one thing that is not known is whether this enhancement is caused by the velocity fluctuations or the pressure fluctuations. For this reason it is important to know the acoustic behavior in the test section. The solution to this problem is derived by solving (A.1)

$$\nabla^2 p' = \frac{1}{a^2}\frac{\partial^2 p'}{\partial t^2} \tag{A.1}$$

where the pressure is assumed to be an imaginary exponential function (A.2).

$$p' = A(x,y)e^{i\omega t} \tag{A.2}$$

The substitution of X(x)*Y(y) for A(x,y) allows for the exponential to be divided out and relation (A.3) left.

$$Y\frac{d^2X}{dx^2} + X\frac{d^2Y}{dy^2} = -\frac{\omega^2}{a^2}XY \tag{A.3}$$

This allows for separation of variables with the boundary conditions on the wall being the no slip condition or u' and v' equal to zero. Combined with continuity, the result is the pressure fluctuation at the wall being zero. This allows for the results in (A.4).

$$
\begin{aligned}
f_{nm} &= \frac{a}{2L_1}\sqrt{n^2+m^2\left(\frac{L_1}{L_2}\right)^2} \\
p'_{nm} &\propto \cos\left(\frac{n\pi x}{L_1}\right)\sin\left(\frac{m\pi y}{L_2}\right) \\
u'_{nm} &\propto \sin\left(\frac{n\pi x}{L_1}\right)\sin\left(\frac{m\pi y}{L_2}\right) \\
v'_{nm} &\propto \cos\left(\frac{n\pi x}{L_1}\right)\cos\left(\frac{m\pi y}{L_2}\right)
\end{aligned}
\qquad \text{(A.4)}
$$

These results allow for the acoustic behavior inside the test section to be determined and at what frequencies the resonance should theoretically happen.

A comparison between the expected resonance frequencies and the actual valued is included in Table A.1.

**Table A.1**: Comparison of calculated resonance frequencies to actual resonance frequencies for the 3' x 3' wind tunnel.

| n | m | $f_{calc}$ (Hz) | $f_{act}$ (Hz) |
|---|---|---|---|
| 1 | 0 | 189 | 200 |
| 1 | 1 | 267 | 284 |
| 2 | 0 | 378 | 386 |
| 2 | 1 | 423 | 436 |
| 2 | 2 | 534 | 542 |

## APPENDIX B: EXPERIMENTAL METHODS

### Flow Visualization Studies

The following are the procedural steps for the flow visualization studies. The steps marked with asterisks (*) are steps only used for the enhancement studies.

1) Install the flat plate in the test section. First, attach two mounting brackets (9 foot long angle sections) into the fiberglass fore and aft of the test section on both sides using bolts. Then mount the test plate itself onto lower side of the mounting brackets using countersunk bolts and nuts (countersunk holes down). Next, attach the center support bracket into the test plate and bolt it into the removable test window on the top of the test section. Finally, attach the trip wire to the leading edge of the plate with two screw in electrical stand offs.

2) Install the smoke generator system. First, mount the smoke manifold on the upper side of the plate. Then, secure the 3" plastic tube between the manifold and the bottom side of the removable test window on the top of test section using a PVC adaptor. Then mount the smoke probe to the top side of the tunnel so that the heat created from the probe will not cause anything to melt or burn, but so that the smoke will enter the PVC adaptor. Then wire the smoke probe to the electrical supply, first between the smoke probe and the coil and then between the coil and the variac, and finally plug the variac into the wall. Next, connect the fluid supply to the smoke probe and the compressed air supply into the fluid reservoir. Ensure that the fluid reservoir is filled with Rosco Fog Fluid. Finally, set the pressure at 60 psi, the variac at 60 Volts, the smoke probe fluid valve at about 1/4 of 1 turn open. (Open the valve near the fluid reservoir and turn the variac on when you are ready to run)

Note: Rosco Fog Fluid was chosen based upon its non toxic nature and limited aroma.

3) Install the 3" foam screen. This is easily accomplished by placing the foam in the diffuser. At that point you can climb into the tunnel and secure the foam against the upstream screen behind the test section. No securing brackets are needed because the foam screen is cut oversize. This will allow the screen to be secured simply by compression of the foam against the walls since this is only for low velocity flows.

4) Set up the optical system. Turn the laser on low power at least 20 minutes before you are ready to run so that it may warm up and ensure that the beam is blocked with a beam stop. Set the optics for the specific test that is being run. The Test Section Modification section gives an overview of this setup. Turn the laser to full power when you are ready to run.

*5) Install the acoustic system. First, install the speaker in lower removable test window. Then, attach the speaker leads from the amplifier to the speaker. Finally, attack the acoustic signal source to the amplifier. This source may be a pure tone signal generator or a white noise generator. It is recommended that if the white noise generator is used, that a band-pass filter be employed to limit the signal to the desired range so that the maximum amount of energy can be put into the flow in that range. Turn on the amplifier when you are ready to run.

6) Place the camera in the desired location. It is recommended that a television screen be employed so that it is easier to view the flow and adjust the focus. It was found that a CCD camera with a 1/500th shutter speed with a SVHS recorder worked best but it appeared that the CCD array was sensitive to electrical spike caused by the start of the tunnel. It was best to plug in the camera once the tunnel was running.

7) Once everything is accomplished and you are ready to start the test, it is time to start the tunnel. This step must be performed with caution. First, ensure that tunnel is **free of any loose tools and/or equipment**. Next, check the pitch indicator on the control panel to ensure that it is at or below zero (the tunnel will not start with a

positive angle on the blades). **Push the start button and as soon as the blades start to turn, you can hear the start, bring the blade up to a positive pitch**. This is important because at a negative pitch the flow is reversed with a large amount of swirl. This will cause the foam screen to become dislodged and the plate will vibrate violently.

8) At this point, all of the equipment can be turned on and the laser turned up to full power (make sure that the vibrating mirror is turned on first).

9) Run the test. To set the desired velocity, make small adjustments at a time. If you over-accelerate the flow, you may need to unload the blades and start over. The foam screen will cause the blades to stall and will limit the upper velocity of the flow.

10) When the test is complete, turn off all equipment (let the laser cool down for 20 minutes before you shut it down), and push the stop button on the control panel to shut down the wind tunnel. These steps can be performed in any order but do not turn off the vibrating mirror before the laser beam is blocked.

11) In order to enhance the flow visualization images, a computer is needed. The VHS or SVHS recorder is plugged into a frame grabber computer board which are available for all types of platforms. For this experiment a Macintosh was available. The software program Quickimage was used to digitize the desired images. Once the images were digitized, Photoshop was used to enhance the image. This was accomplished by multiple adjustments of the brightness and contrast. These images could then be printed or used directly in other applications.

**Pressure Measurements**

The following are the procedural steps for the pressure measurement studies.

1) Install the flat plate in the test section. First, attach two mounting brackets (9 foot long angle section) into the fiberglass fore and aft of the test section on both sides using bolts. Then mount the test plate itself onto lower side of the mounting brackets using countersunk bolts and nuts (countersunk holes down). Next, attach the center support bracket into the test plate and bolt it into the removable test window on the top of the test section. Finally, attack the trip wire to the leading edge of the plate with two screw in electrical stand offs.

2) Install the 3" foam screen. This is easily accomplished by placing the foam in the diffuser and then climbing into the tunnel. At that point you can climb into the tunnel and secure the foam against the upstream screen behind the test section. No securing brackets are needed because the foam screen are cut oversize. This allow the screen to be secured simply by compression of the foam against the walls since this is only for low velocity flows.

3) Install the pressure measurement system. First screw the condenser microphone into the adaptor and then into the pre-amplifier cable. This cable is then attached into the Brüel and Kjaer high resolution signal analyzer. The microphone is then run into the test section through the small hole in the center of the removable test window on the top of the test section. Then place the microphone at the desired location on the testing side of the test plate. Do not turn on the signal analyzer before the microphone is connected.

4) Once everything is accomplished and you are ready to start the test, it is time to start the tunnel. This step but must be performed with caution. First, ensure that tunnel is **free of any loose tools and/or equipment**. Next, check the pitch indicator

on the control panel to ensure that it is at or below zero (the tunnel will not start with a positive angle on the blades). **Push the start button and as soon as the blades start to turn, you can hear the start, bring the blade up to a positive pitch**. This is important because at a negative pitch the flow is reversed with a large amount of swirl. This will cause the foam screen to become dislodged and the plate will vibrate violently.

5) At this point, all of the equipment can be turned on.

6) Run the test. To set the desired velocity, make small adjustments at a time. If you over accelerate the flow, you may need to unload the blades and start over. The foam screen will cause the blades to stall and will limit the upper velocity of the flow.

7) Record all data on either the plotter or the digital tape recorder. This will allow for further study after the test.

8) When the test is complete, turn off all equipment, and push the stop button on the control panel to shut down the wind tunnel. These steps can be performed in any order.

9) Once the test is over, the data saved to the digital tape recorder can be transmitted to a computer through a GPIB connector. This will allow for data analysis and presentation.

## APPENDIX C: RECORD OF VIDEO TAPE RECORDINGS

The following table is a record of the video tape recordings made for this project. The pictures of the hairpin vortices were taken off of this tape via the method described in Appendix B. If more footage is needed, a copy of the SVHS tape can be made available by contacting Dr. Mitsuru Kurosaka in the department of Aeronautics and Astronautics.

NOTES:

* Stream - Streamwise view, Downstrm - Downstream view, Upstream - Upstream view

** None - No acoustic enhancement, White - White noise enhancement

*** File #2 contains no relevant information

**Table C.1**: Summary of taped files on SVHS video tape

| Date | Run # | V (m/s) | x (m) | view* | noise** |
|---|---|---|---|---|---|
| 11/2/93 | 1 | 3.0 | 2.0 | stream | none |
| 11/2/93 | 2 | 4.0 | 2.0 | stream | none |
| 11/2/93 | 3 | 5.0 | 2.0 | stream | none |
| 11/2/93 | 4 | 3.0 | 2.0 | downstrm | none |
| 11/2/93 | 5 | 4.0 | 2.0 | downstrm | none |
| 11/2/93 | 6 | 5.0 | 2.0 | downstrm | none |
| 11/2/93 | 7 | 3.0 | 2.0 | upstream | none |
| 11/2/93 | 8 | 4.0 | 2.0 | upstream | none |
| 11/2/93 | 9 | 5.0 | 2.0 | upstream | none |
| 11/2/93 | 10 | 3.0 | 1.0 | stream | none |
| 11/2/93 | 11 | 4.0 | 1.0 | stream | none |
| 11/2/93 | 12 | 5.0 | 1.0 | stream | none |
| 11/2/93 | 13 | 3.0 | 1.0 | downstrm | none |
| 11/2/93 | 14 | 4.0 | 1.0 | downstrm | none |
| 11/2/93 | 15 | 5.0 | 1.0 | downstrm | none |
| 11/2/93 | 16 | 3.0 | 1.0 | upstream | none |
| 11/2/93 | 17 | 4.0 | 1.0 | upstream | none |
| 11/2/93 | 18 | 5.0 | 1.0 | upstream | none |

**Table C.2**: Table C.1 Continued

| Date | Run # | V (m/s) | x (m) | view * | noise ** |
|---|---|---|---|---|---|
| 11/9/92 | 1 | 4.0 | 2.0 | stream | none |
| 11/9/92 | 3*** ≐ | 4.0 | 2.0 | stream | white |
| 11/9/92 | 4 | 3.0 | 2.0 | stream | none |
| 11/9/92 | 5 | 3.0 | 2.0 | stream | white |
| 11/9/92 | 6 | 3.0 | 2.0 | downstrm | none |
| 11/9/92 | 7 | 3.0 | 2.0 | downstrm | white |
| 11/9/92 | 8 | 4.0 | 2.0 | downstrm | none |
| 11/9/92 | 9 | 4.0 | 2.0 | downstrm | white |
| 11/9/92 | 10 | 3.0 | 2.0 | upstream | none |
| 11/9/92 | 11 | 3.0 | 2.0 | upstream | white |
| 11/9/92 | 12 | 4.0 | 2.0 | upstream | none |
| 11/9/92 | 13 | 4.0 | 2.0 | upstream | white |
| 11/9/92 | 14 | 3.0 | 1.0 | stream | none |
| 11/9/92 | 15 | 3.0 | 1.0 | stream | white |
| 11/9/92 | 16 | 4.0 | 1.0 | stream | none |
| 11/9/92 | 17 | 4.0 | 1.0 | stream | white |
| 11/9/92 | 18 | 3.0 | 1.0 | downstrm | none |
| 11/9/92 | 19 | 3.0 | 1.0 | downstrm | white |
| 11/9/92 | 20 | 4.0 | 1.0 | downstrm | none |
| 11/9/92 | 21 | 4.0 | 1.0 | downstrm | white |
| 11/9/92 | 22 | 3.0 | 1.0 | upstream | none |
| 11/9/92 | 23 | 3.0 | 1.0 | upstream | white |
| 11/9/92 | 24 | 4.0 | 1.0 | upstream | none |
| 11/9/92 | 25 | 4.0 | 1.0 | upstream | white |